

Study of the Anthropogenic Impact in Farmington Bay through Freeze Core Analysis

Nathan Gunnell

Brigham Young University

2020

Introduction

Farmington Bay is a brackish to fresh water arm of the Great Salt Lake. Located directly east of Antelope Island in the southeast sector of the Great Salt Lake, it covers an area of about 95 mi² (260 km²) (Fig. 1). Farmington Bay is bounded on the west by a small causeway built in 1952 to prevent wastewater from reaching Gilbert Bay (Table 1), and on the north by an automobile causeway to Antelope Island which essentially isolate the bay from the rest of the lake. The bay contains a waterfowl management area which is home to many species of birds (Wurtsbaugh et al., 2002) and is part of the overall Great Salt Lake ecosystem that receives industrial, urban, mining, and agricultural discharge from nearly 2 million people that live along the Wasatch Front (Naftz et al., 2008). Farmington Bay is of particular interest because it receives significant nutrient discharge from several wastewater treatment facilities in Salt Lake and Davis Counties (Wurtsbaugh and Marcarelli, 2006), and indirectly from Utah County via Utah Lake and the Jordan River. Farmington Bay experiences many of the same effects of nutrient loading observed in similar waterbodies.

Farmington Bay maintains salinity values of 3-5% compared to 11-28% in the rest of the lake (Goel and Myers, 2009). This freshening occurred as the result of hydrodynamic isolation due to the causeway construction driving nutrient concentrations to increase and salinity to decrease (Wurtsbaugh and Marcarelli, 2006). Farmington Bay receives the majority of its water from the Jordan River, an outlet from nearby Utah Lake, which transports nutrients from wastewater treatment facilities into the bay. Before reaching the bay, the river passes through a series of wetlands designed to retain most of the nutrients and prevent them from reaching the bay (Wurtsbaugh and Marcarelli, 2006).

Naftz et al. (2000) suggested that the sediment deposited in Farmington Bay before the early 1900s was relatively uncontaminated (defined in the study as low concentrations of Cd, Cu, Pb, Zn, N, organic C, and P). From there, the study showed the level of contamination steadily increased over time and from 1979 to 1998 the most contaminated sediment was deposited. Wurtsbaugh et al. (2002) demonstrated that Farmington Bay is one of the most polluted water bodies in Utah and that phosphorous levels in the bay are 8-times higher than the level required for it to be considered eutrophic. The eutrophication of the bay began to increase rapidly after the completion of the causeways, even with the construction of an additional wastewater treatment facility in Salt Lake City (Leavitt et al., 2012) and has contributed to recent outbreaks of harmful algal blooms.

This study employs mineral, isotopic, and chemical records from Farmington Bay freeze cores that will provide evidence of environmental changes over time as a result from human activity. Isotopic studies will provide a temporal framework using ²¹⁰Pb, nutrient sources with analysis of ¹⁵N, and changes in environment with ¹³C. Bulk mineralogy may also reveal changes in sediment sources and changes in overall water quality. Finally, examining concentrations of nutrients and trace metals in pore water over time may provide information on the timing and magnitude of human influence on the bay. Table 1 shows major human activities occurring over the past 150 years that may be recorded in the sediment. The data acquired in this study will be used to

construct a stratigraphic record showing the impact human activity in the area over the past several decades and where possible, they will be tied to the events in Table 1.

Table 1. Timeline of important events that have contributed to contamination and eutrophication in Farmington Bay. Adapted from Leavitt et al. (2012) and Wurtsbaugh (2012).

Year	Event
1847	Salt Lake Valley settled by Mormon pioneers
1863	Bingham Mine begins mining copper
1885	Surplus Canal built re-routing the Jordan River into Gilbert Bay instead of Farmington Bay
1889	Sewer line completed from Salt Lake City to the Jordan River
1892	Gold, lead and silver smelter begins operation
1911	Outlet Sewage Canal completed that dumped wastewater from Salt Lake City directly into Farmington Bay (replaced sewer line to Jordan River)
1916	Cudahy Packing Company begins discharging meat waste into Jordan River and Farmington Bay
1922	Oil drain connected to the sewage canal
1930	Construction of the Farmington Bay Waterfowl Management Area, designed to prevent Jordan River nutrients from reaching the Bay by retaining them in wetlands
1952	Southern causeway completed, separating Gilbert Bay and Farmington Bay on the south end
1959-1962	Formation of sewerage districts to begin treating and discharging wastewater into Farmington Bay
1963	Great Salt Lake at lowest recorded level (1277.8 m)
1965	Additional wastewater treatment facility constructed in Salt Lake City
1969	Completion of automobile causeway to Antelope Island
1984	Great Salt Lake flood stage (1282.86 m); Automobile causeway flooded until 1989
1989	Phragmites introduced in the environment as water level recedes
1992	Automobile causeway rebuilt
2002	Wetlands restoration project along the Jordan River begins
1990-Present	Water level of the Great Salt Lake steadily receding

Methods

Field Methods

Freeze cores were collected from Farmington bay in late May of 2018 (Fig. 1) using a device similar to (National Lacustrine Core Facility (LacCore) : University of Minnesota). The first core (FB-1) was taken near the inlet of the oil drainage canal and historical sewage canal and the

second core (FB-2) was taken close to the wetlands where the Jordan River enters the bay (Table 2). As the standing water is very shallow in the bay (5-10 cm at the time of collection), an air boat was used to access the core sites. The corer was pressed into the soft sediment by hand as far as possible. The sediment freezes to the corer and retains its position as it is retrieved. This is advantageous because it significantly reduces compaction of soft sediment and retains visual stratigraphic integrity (Fig. 2). The core was transported in a cooler with dry ice and stored at BYU in a vacuum sealed bag in a freezer at -20°C .

Lab Methods

Sample preparation of frozen core, taking care to avoid cross contamination, was achieved by cutting a 4 cm section of the core with a band saw and cutting it into 1 cm pieces which were then placed in individual 50 mL plastic centrifuge tubes. The individual samples were measured and weighed to obtain their dimensions and mass. Once the samples were measured, they were freeze dried. Once completely dry, the samples were weighed again to calculate dry bulk density and porosity. The sediment from each sample was then disaggregated by hand with a mortar and pestle in preparation for the different analyses. Separate aliquots for pore water analysis were recovered as discussed below.

Determining Core Ages

The first step in constructing the stratigraphic record is to constrain the ages of the cores with respect to depth. Analysis of the ^{210}Pb isotope can give an idea of the age of the sediment based on the ratio of supported vs. unsupported ^{210}Pb activity from ^{238}U decay using the methods described by Appleby (2001). Twenty samples from each core (alternating every other or every third cm) were sent to the Science Museum of Minnesota where the difference between supported and unsupported ^{210}Pb was measured with alpha spectrometry of ^{210}Po to provide age estimates at various depths of the cores using the constant rate of supply (CRS) model (Appleby, 2001). ^{210}Po is the daughter of ^{210}Pb and having a much shorter half-life (138 days vs 22.3 years), it will have an activity equal to its parent. Another advantage of counting ^{210}Po is that it is an alpha emitter and the counting efficiency is very high, compared to the counting efficiency of beta emissions of ^{210}Pb , increasing analytical precision and detection limits.

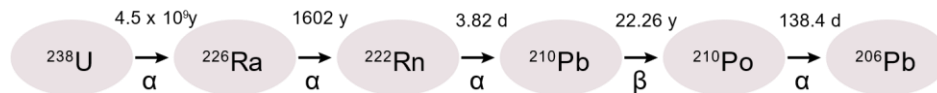


Figure 3. Simplified representation of the decay path if ^{238}U to ^{210}Pb showing the half-lives and decay type of each isotope

Minerology

A small amount of sediment from each sample was placed in zero background holders and analyzed by X-ray diffraction (XRD) from 5 to $65^{\circ} 2\theta$ using Cu radiation with a Rigaku MiniFlex 600 spectrometer at Brigham Young University. Results were analyzed by Rietveld analysis using the PDXL2 software package, which provides a semi-quantitative representation

of mineral content in each sample. The samples were initially run at 0.2-degree intervals at 1 second per interval. To decrease the background noise, a few samples were run for 2-4 seconds per interval, however the resulting background noise was relatively unaffected. Results of the Rietveld analysis returned an average R_{wp} value of 15.9% and S value of 1.65. The minerals included in the analysis were quartz, calcite, aragonite, dolomite, albite, and illite with a corundum internal standard. The relationship between calcite and aragonite is particularly significant as these minerals are $CaCO_3$, however, they form in different chemical structures based on environmental conditions (Wray and Daniels, 1957; Fyfe and Bischoff, 1965; Ogino et al., 1987).

Rock-Eval (Pyrolysis)

About 70 mg of sediment per sample was analyzed for organic and inorganic carbon content through pyrolysis. Each sample was heated initially to about 400°C at which temperature the hydrocarbons are evolved. After this initial heating, the temperature is increased to 700°C which produces CO_2 through the breakdown of carbonate materials. Details of the heating schedule can be found in Hudson et al. (2019). The hydrogen index (HI) is measured in this second heating stage and can give information into the carbon source of the sediment, whether it is organic (vascular plants, etc.) or inorganic (algae) (Espitalie et al., 1985; Peters, 1986; Baskin, 1997; Dembicki, 2009; Hudson et al., 2019).

$\delta^{15}N$ and $\delta^{13}C$ isotopes

For the $\delta^{13}C$ value of organic material to be analyzed, carbonate was removed by treatment with 10% HCl following SIRFER protocol (a process described by Verardo et al. (1990)). About 100 mg of sediment per sample was sent to the SIRFER lab at the University of Utah to measure the $\delta^{13}C$ and $\delta^{15}N$ values of organic matter. The $\delta^{15}N$ values provide insight to the main source of nitrogen in the environment (Delwiche and Steyn, 1970; Wada et al., 1975; Clark and Fritz, 1997; Bateman et al., 2005) and the $\delta^{13}C$ value illustrates the plant-mineral-water interaction (Fig. 4).

Pore-Water

To obtain pore-water data, separate samples were cut from the core. The samples were weighed and pore water extracted by dilution with Milli-Q water, centrifuged, filtered, and analyzed by inductively coupled plasma optical emission spectrometry (ICP-OES) and ion chromatography (IC) analysis at Brigham Young University to determine the concentrations of cations, anions, and trace elements. After extraction, remaining sediment was dried and re-weighed to obtain proper dilutions.

Of particular interest is the concentration of phosphorous as it is a major nutrient that contributes to eutrophication (Leavitt et al., 2012), which may lead to harmful blue-green algae blooms (Moser et al., 2012). Trace metals reflect the impact of nearby Bingham Mine which began copper mining in the early 1860's and the oil drain from the North Salt Lake refineries. Wurtsbaugh (2012) found significant increases in Cu, Pb, Zn, and Hg concentrations in Gilbert Bay cores beginning in the late 1800's. He also found increases in those same elements in a core

taken near the location of FB-1, located near the inlet of the wastewater/oil drain canal, which occurred around 1950. Cu, Pb, Zn, and Hg concentrations were not measured as part of this study, however, other trace metals were investigated.

Analysis of pore-water chemistry was done using Geochemist's Workbench (GWB). The software can be used to create models or diagrams useful in explaining and understanding measured water chemistry data (Cleverley and Bastrakov, 2005). In this study, the pore water chemistry data was entered into the Geochemist's Spreadsheet (GSS) which was used to generate Stiff and Piper diagrams.

Most major cation and anion concentrations were measured through ICP and IC analysis, however, there was insufficient sample for HCO_3^- by titration. The concentration of HCO_3^- was calculated by charge balance with the other major ions. Six samples from each core were selected to illustrate changes in water chemistry over time as a result of human activity, one sample from the top and bottom, one prior to the completion of the sewage canal in 1911 and one after, and one from before the construction of the southern causeway as well as one after the northern causeway was completed. Stiff and Piper diagrams were created for comparison of cations and anions with respect to depth.

Smear Slides

A very small amount of sediment was used to make smear slides for each sample. The slides were mounted with ZRAX which has a high refractive index, making the grains easier to see and permitting qualitative description of the sediment, including diatoms, grain types and sizes, nature of organic matter, etc. (Schnurrenberger et al., 2003; Myrbo et al., 2011). The presence of these organisms is significant, as changes in environmental conditions (salinity, eutrophication, etc.) affect how well populations of different species survive within that environment.

Results

^{210}Pb

Figure 5 presents the results of ^{210}Pb analysis of sediment, for cores FB-1 and FB-2. Neither of the ^{210}Pb activity graphs (Fig. 5A and 5B) follow a very linear pattern, which Appleby (2001) explained could be due to increased sedimentation rates, variation in sediment focusing, changes in normal sediment accumulation processes, or physical, biological, or chemical mixing. The relationship for FB-2 followed the expected asymptotic form with the supported ^{210}Pb abundance (Fig. 5B), but FB-1 never quite reached the point where it became asymptotic (Fig. 5A). The base of unsupported ^{210}Pb line for FB-1 was drawn at 17 cm which has a calculated date of about 1935 (Fig. 5C).

The base of the supported ^{210}Pb line for FB-2 was picked at about 30 cm and had a calculated date of 1920, nearly 100 years prior to collection of the core (Fig 5D). Because the base of the unsupported ^{210}Pb dating horizon has been reached, further constraints on the age of deeper horizon is not possible except by extrapolation.

Because of the discrepancy in ^{210}Pb activity in FB-1, ages at depths below 15-18 cm will not be as precise as those observed in FB-2. Pending further analysis of additional subsamples for ^{210}Pb and ^{137}Cs will better constrain the age-depth relationships in the cores. If results from this further analysis do not provide more accurate age constraints at lower depths, ages dating back to 1850 may need to be extrapolated using an average sedimentation rate. However, since the pioneers arrived in the valley in 1847, the need to extrapolate is relatively inconsequential because it would have taken some time for human development to impact the bay.

$\delta^{15}\text{N}$

Results show that approximately 100 years ago, a dramatic shift in the source of nitrogen is recorded (Fig. 6). The values of $\delta^{15}\text{N}$ for both cores change from about 6-7‰ to around 10‰. Figure 4 (Clark and Fritz, 1997) shows nutrient sources based on $\delta^{15}\text{N}$ values of a sample. The shift in the $\delta^{15}\text{N}$ values indicates a change in nutrient source from influenced by organic nitrogen to manure and wastewater dominated. The abrupt change in value is particularly noticeable in FB-2. This excursion appears to be a response to the completion of the sewage canal in 1911 (Leavitt et al., 2012) when raw sewage was diverted into Farmington Bay.

Core FB-1 also becomes more enriched from bottom to top; however, it shows more variability in $\delta^{15}\text{N}$ values prior to reaching and maintaining values of 10‰. There appears to be a minor enrichment period in the early 1900's followed by gradual depletion back to about 7‰. The $\delta^{15}\text{N}$ value of the core finally is enriched and stabilized to about 10‰ beginning around 1970 with the isolation of the bay. While FB-2 quickly reflected the change in nutrient source being input into the bay, FB-1 may have been more subject to mixing with the main body of the lake, not fully reflecting the new sewage nutrient source until the completion of the southern and automobile causeways (Fig. 1).

$\delta^{13}\text{C}$

While the isotopic changes between the two cores were similar for nitrogen, there were significant variations between FB-1 and FB-2 with respect to the ^{13}C isotope (Fig 7). The bottom of FB-2 showed a depletion value of -22‰. Moving up along the core, the value fluctuated between -21‰ and -23‰ and returned to -22‰ at the top of the core. FB-1 had a starting value closer to -20‰ and became slightly more enriched to about -18‰ between 1925 and 1970 before returning back to its original value. Then in the early 1990's, the $\delta^{13}\text{C}$ value enriched steadily to a value close to -15‰ at the top of the core. With such distinct differences between the two cores, it is important to investigate why they are so different.

Pore-Water

Major Elements

After calculating and adding HCO_3^- to the dataset, the overall charge of the system became well-balanced, especially at the top of the core. The charge imbalance error did increase slightly with respect to depth, but the values were still low. The speciation results showed that the molality of aqueous species decreased in all the major ions. The molality of K^+ , Ca^{2+} , Mg^{2+} , SO_4^{2-} , and HCO_3^- species all decreased by a factor of 10 while the molality of Na^+ and Cl^- species decreased

by a factor of 15 from the bottom of the core to the top. These results are supported by the Stiff diagrams (Fig. 8) which show the concentrations of the cations and anions decreasing upward in the core. The twelve samples plot almost on top of one another on the Piper diagram (Fig. 9) indicating that while the concentrations of the major ions are decreased, the relative ratios between the ions remained the same except for a slight deviation at the top sample of each core where there is a slightly higher Ca concentration.

Overall, the diagrams and data obtained from GWB illustrate the environmental response to the construction of the causeway and other human impacts in the bay. The decrease in concentrations of major cations and anions observed in the Stiff diagrams (Appendix A) is significant because they indicate a freshening as a result of the completion of the sewage canal in 1911. It was expected to observe a change like this once the bay was completely isolated due to the construction of the causeways, however it appears that the input of another freshwater source, albeit wastewater, caused the water in the bay to begin to freshen with respect to the major ions. The completion of the causeway in 1969 appears to have accelerated the freshening process.

Phosphorus

While the molality of major ions decreased, molality of total P increased by a factor of 10 from the bottom to the top of the core. From Figure 10, it is also observed the phosphorous concentration began increasing slowly in FB-1 at a depth to the construction of the sewage canal into Farmington Bay in 1911. In FB-2, the concentration begins to increase in the mid to late 1940's. By around 1970, the increase in concentration appears to accelerate and around 1990 the phosphorus concentrations of both cores spike sharply. At the top of the core, the phosphorous concentration decreases which is likely due to diffusion within the pore water. Additionally, phosphate concentrations follow the same general curve as phosphorus. The value remained below the detection limit until about 1915 in FB-1, and until about 1950 in FB-2. Each sample was also tested for nitrate; however, for all but one sample, nitrate was below the detection limit.

Trace Metals

From the trace metal data obtained, no significant increase in concentration for any metal was observed in Farmington Bay until after 1980 indicating that the waste from Bingham Mine was limited to Gilbert Bay and that the contaminants from the oil drain were limited to those more common trace metals discussed by Wurtsbaugh (2012). Additional trace metal concentrations began to increase in the 1980's and especially the 2000's. Three main trends were found after observing the data for trace metals: elements whose concentration increased over time, elements whose concentration decreased over time, and elements that increased along both cores over time, then continued to increase in FB-2 but decreased in FB-1.

Mn and Ni were the only elements to follow this first trend (Fig. 11). Both maintain relatively low concentrations until the 1990's when a sudden increase in concentration is observed. Since this increase correlates to the time when water level began receding, and because the concentrations are higher in FB-1 than FB-2, it could be that the oil drain contained Mn and Ni as well, just too small of an amount to be observed until the water level began to decrease. Al, Fe and Ti followed the same pattern as Mn and Ni. The concentrations remained near 0 from the

bottom of the core until the late 1980's/early 1990's. The concentrations then increased in both cores for about 10 years, however, while that increase continued in FB-2, they decreased all the way to near 0 in FB-1 (Fig. 12). Sr, Sb and As all show a general, though subtle, decrease in concentration over time, whereas B and Li begin at high concentrations at the bottom of the core and steadily decrease until the top of the cores where the concentration is close to 0 (Fig. 13). Both B and Li are closely associated with briny or marine environments (Nable et al., 1997; Kavanagh et al., 2018) and follow the same pattern as the major elements that decreased in concentration especially after the sewage canal and causeways were built. This would indicate that these elements are connected to the bay's natural environment and not to human influence.

Minerology

A total mineralogy composition chart was created with the results from the Rietveld analysis of the XRD data (Fig. 14). When observed individually, not much change in composition was observed in quartz, albite, dolomite, or the clay minerals from the bottom to the top of either core. However, in both FB-1 and FB-2 (though more apparent in FB-2), at the depth corresponding to the construction of the sewage canal a compositional shift occurs in both calcite and aragonite as shown in Figure 15. Until that point, the percent of calcite in the sediment had been slowly increasing from about 17% at the base of the core all the way to near 50%. Once raw sewage began entering the bay, the amount of calcite shows a decrease from 50% to about 15% while the aragonite composition in the sediment shows an increase from 10% to about 20% only about 7 cm further up the core. Both minerals remained at this new composition, with a few minor fluctuations, the rest of the way up the core. It was suspected that the wetlands built in 1930 may have acted as a sediment trap, however, while there is a very minor increase in the percentage of clay composition at that time (< 5%) the other minerals exhibit very little change.

Pyrolysis

Results from the Rock-Eval pyrolysis indicate a slow increase in HI values beginning in the 1910's in FB-1 and a sudden spike in values beginning thirty years ago in both cores (Fig. 16), although the value increases significantly more in FB-1 than FB-2. The HI values increased from an average around 100 to as much as 490 in FB-1 and up to 360 in FB-2. These higher HI values could signify the increasing presence of algae as early as 1990.

Smear Slides

The images shown in Appendix B illustrate the variation in diatom presence with respect to depth across both cores. In FB-1, a high abundance of diatoms is observed in the upper 7 cm of the core, after which the number of diatoms steadily decreases until after 13 cm (around 1970) the presence of diatoms is no longer apparent. From 13 cm to about 30 cm, the samples are composed largely of inorganic matter, although there is a fairly high amount of organic (mostly plant) material observed as well. A small number of diatoms reappear after 30 cm (about 1900) and are seen through the remainder of the core. A very high number of diatoms is also observed in the top of the core of FB-2. Similar to FB-1, by 1970 the presence of diatoms disappeared and until a depth of 29 cm (about 1922) the sediment contained mostly inorganic and plant-based

material. However, from 29 cm until the bottom of the core, an even greater abundance of diatoms than what was observed in FB-1 is seen in FB-2.

The presence of diatoms at the base of both cores is surprising. It was originally hypothesized that the bay was too saline prior to the construction of the causeway to provide a suitable environment for diatoms to exist. Clavero et al. (2000) discussed that 7.5% salinity is a natural barrier to survival of diatoms and few species have adapted to survive in hypersaline environments. However, the diatom community was present, albeit small, in both cores until the early 1900's. This could imply that the disappearance of diatoms correlates to the completion of the sewage canal. Studies done by Michels (1998) and Kim et al. (2008) have shown that while some diatom species can survive in an effluent-rich environment, others cannot. Since the disappearance of the diatom species in Farmington Bay correlates with the inflow of raw sewage, we can presume that such an effluent-rich environment was not conducive to the native diatom species.

The re-emergence of the diatoms around 1970 corresponds to both the completion of the automobile causeway as well as the construction of the secondary wastewater treatment facility in Salt Lake which stopped the discharge of raw sewage into the bay (Wurtsbaugh, 2012). However, the diatom population seems to have remained small until about 1990, just after the bay reached its highest water level, when the number of diatoms in each sample increases dramatically. These results could indicate that sewage content, in addition to salinity, plays a large role in the stability of the diatom population.

Discussion

Environmental Isotopes

From the $\delta^{13}\text{C}$ results, an initial hypothesis is that the excursion near the top of FB-1 is related to a change in vegetation type. The -22‰ value reflects a $\delta^{13}\text{C}$ value found in C3 plants while the lower value of -15‰ is more representative of C4 plants. The enrichment of $\delta^{13}\text{C}$ begins at a depth that corresponds to about 1990, at which time the lake level began receding and the invasive phragmites grass was introduced. Since grasses are a common type of C4 plant (Clark and Fritz, 1997), phragmites might be a C4 plant and thus contribute to the enrichment of $\delta^{13}\text{C}$ in the core. However, studies have shown that while some young phragmites leaves experience a C4 photosynthetic process, phragmites itself is a C3 plant (Antonielli et al., 2002; Saltonstall et al., 2005; Liu et al., 2015).

Upon further examination of the core data, it appears that the trend toward a more enriched $\delta^{13}\text{C}$ value began in the early 1920's. Figure 7 shows the enrichment process was interrupted around 1970, corresponding to the time the automobile causeway was completed. However, once the water level began receding in the late 1980's/early 1990's, the enrichment process began again, continuing to the -15‰ value seen today. The initial enrichment of $\delta^{13}\text{C}$ in the early 1920's may be a result of the oil drain that was connected to the sewage canal in 1922 from the refinery in North Salt Lake (Wurtsbaugh, 2012). If the oil drain contained a high amount of dissolved inorganic carbon (DIC) or organic carbon, it would have an enriching effect in the area in which it discharged. This would have continued until the causeway was completed in 1969. The

isolation of the bay would have resulted in the fresh water from the Jordan River, more depleted in $\delta^{13}\text{C}$ as a result of fractionation through photosynthesis of C3 plants while passing through the wetlands, mixing more with the water discharging from the oil drain. This, along with rising water levels would cause the $\delta^{13}\text{C}$ to be more depleted in FB-1. The Great Salt Lake reached flood stage in 1984, resulting in the flooding of the automobile causeway (Table 1). The causeway remained flooded until 1989 and was rebuilt in 1992 after the water had receded. As the water level receded, the area in which the oil drain discharged into the bay became partially disconnected from the rest of the bay during low water seasons (Wurtsbaugh, 2012). This would allow FB-1 to once again become enriched in $\delta^{13}\text{C}$ (Fig. 7). However, in a study by Whittaker et al. (1996), it was shown that most oils range from -26.8‰ (heavy) to -28.8‰ (light) meaning that unless there was a very high amount of DIC mixed with the waste from the refineries, there likely was not enough enrichment from the oil drain to produce the excursion.

A more probable explanation could be that the initial excursion correlates to the sewage from the canal. The ^{210}Pb results for FB-1 aren't as precise as for FB-2 so there is more uncertainty in age estimates. The sewage dumped into the bay from the newly constructed canal would have contained algae. This is supported both by the disappearance of diatoms, which would have been outcompeted for nutrients by the introduction of algae, at the time of the sewage canal construction and the contemporaneous increasing HI values observed in Figure 16. It is possible that algae introduced to the environment contained a $\delta^{13}\text{C}$ signature lower than what previously existed in the bay. Kokke (1984) and Fry (2006) showed that various types of algae can have values between -11‰ and -20‰. France (1995) provided a distribution of $\delta^{13}\text{C}$ values of benthic and planktonic algae in both fresh and marine aqueous environments (Table 2).

Table 2. Ranges of benthic and planktonic algae in marine and fresh water as described by France (1995).

		$\delta^{13}\text{C}$ (‰)		
		Low	High	Mean
Benthic	Marine	-30	-4	-17
	Freshwater	-36	-20	-26
Planktonic	Marine	-32	-16	-22
	Freshwater	-20	-44	-32

Furthermore, because both the hydrogen index and $\delta^{13}\text{C}$ values follow the same general curve in FB-1, they were also plotted against each other. The resulting scatterplot (Fig. 17) showed a strong correlation between HI and $\delta^{13}\text{C}$ in FB-1 with an R^2 value of 0.54. A strength of correlation test returned a p-value of 0.0001 signifying a very strong correlation between the two values. No correlation was observed between the two datasets in FB-2 ($R^2 = 0.00$, $p = 0.78$). This indicates that the increase in organic carbon heavily influenced the enrichment of $\delta^{13}\text{C}$ in FB-1 meaning the excursion observed in Figure 7 is likely driven by algae.

Of additional interest is to understand why the sewage canal/oil drain caused such a difference at FB-1 in the $\delta^{13}\text{C}$ results, but not in $\delta^{15}\text{N}$, particularly because it was FB-2 that showed a greater response to the input of wastewater, and FB-1 is located closer to the outlet of the sewage canal. The primary source of ^{13}C in the sewage canal/oil drain differed from that of the Jordan River and of the bay itself. However, the source of ^{15}N in the sewage canal likely didn't differ far from that of the Jordan River as wastewater was being discharged into the Jordan River as early as 1889. At that time though, much of the Jordan River was being diverted into Gilbert Bay, implying that wastewater from the Jordan River wouldn't have had much a significant impact in Farmington Bay until being re-diverted from Gilbert Bay back to Farmington Bay in 1930. Additionally, wastewater may not have been the only source causing enrichment in ^{15}N . In 1916, a meat packing facility was opened by the Cudahy Packing company which began discharging excess waste into both the Jordan River and Farmington bay (Strack, 2019). This could have contributed to the larger excursion in $\delta^{15}\text{N}$ value observed in FB-2.

To determine the extent of the impact the sewage had on the calcium carbonate composition, the values of calcite and aragonite were plotted against the $\delta^{15}\text{N}$ to see if there was any correlation between the source of nitrogen entering the system and the form of calcium carbonate (Figure 18). The resulting plot for FB-2 showed a fairly strong correlation of the relationship between $\delta^{15}\text{N}$ and calcium carbonate with an R^2 value of 0.59 ($p = 1.17 \times 10^{-5}$) and 0.50 ($p = 0.0001$) for calcite and aragonite, respectively. This indicates that as $\delta^{15}\text{N}$ increased in the bay, calcite became less stable while the stability of aragonite increased in the new environment. After adding the $\delta^{15}\text{N}$ values for FB-1 as well, the R^2 value decreased to about 0.40 ($p = 3.15 \times 10^{-6}$) for both calcite and aragonite. FB-1 was subject to mixing with Gilbert Bay until the southern causeway was completed and the $\delta^{15}\text{N}$ values didn't reach its value of 10‰ until after both the southern and northern causeways were built.

Pore-water Geochemistry

The initial increase in phosphorus concentration in FB-1 appears to be a result of the sewage canal; however, that same rise in concentration did not appear in FB-2 until about 30 years later even though the $\delta^{15}\text{N}$ value increased to a level indicative of sewage. This can likely be attributed to the waste dumped into the Jordan River from nearby slaughterhouses. That waste would carry a $\delta^{15}\text{N}$ signature similar to that of sewage (Minagawa and Wada, 1984) and the phosphorus in the Jordan River may have been consumed while passing through wetlands before reaching the core site. The increase in phosphorus at FB-2 correlates with the completion of the southern causeway which was built to prevent wastewater from reaching Gilbert Bay (Leavitt et al., 2012). This would have prevented the phosphorus coming into the bay near FB-1 from dispersing into Gilbert Bay, thus allowing more phosphorus to reach FB-2. The phosphorus concentration further increased once the bay was further isolated with the construction of the automobile causeway to Antelope Island. The formation of wastewater treatment facilities throughout the 1960's likely contributed to the increasing concentration as well. The significant spike in concentration observed beginning in 1990 corresponds to the receding water level of the bay and the Great Salt Lake. As additional wastewater was continually discharged into the bay,

and as the water level continued to decline, the concentration of phosphorus in the bay would increase.

Result from pyrolysis are consistent with the high phosphorus levels observed near the top of the cores as well. Figure 19 indicates a strong correlation between phosphorus concentration and HI at FB-1 ($R^2 = 0.66$, 5.92×10^{-9}) Although the correlation at FB-2 is not as strong ($R^2 = 0.33$, $p = 0.0003$), it is still significant and the lower correlation could be a result of water in the bay mixing with the fresh water entering from the Jordan River. The overall response of the HI indicates that as phosphorus concentration increased with the decline in water level in the bay, it provided an environment compatible for enhanced eutrophication.

Summary

Overall, the data points to 3 major human caused/influenced factors that have contributed to the current environmental state of Farmington Bay. The first was the construction of the sewage canal in 1911. The effect the canal was found to have on the bay was significantly greater than originally expected. This secondary input of freshwater into the bay began the freshening process over 50 years before the bay become isolated from the rest of the Great Salt Lake. Moreover, the nutrients input into the bay from the sewage canal initiated a localized response with respect to carbon and a $\delta^{15}\text{N}$ shift observed throughout the bay. This influx of new nutrients likely led to the termination of the already limited diatom population in addition to priming the environment for eutrophication.

Second, the mixing of water from Farmington Bay with the Great Salt Lake was all but eliminated due to the construction of the southern causeway and the northern, automobile causeway. This isolation began a trend of increased phosphorus concentration and accelerated the freshening process started by the sewage canal. Once the bay was isolated, the salinity levels dropped to the 3-5% values observed today. The less saline water also allowed for the reappearance of the diatom population.

Finally, after the lake reached its high stand between 1984 and 1989, a period of drought coupled with an increase of water diverted from the Jordan River for commercial and agricultural use have led to substantial drop in water level, thereby allowing the drastic rise in concentration of elements in the bay. With the primary input water sources of the bay being the Jordan River and processed wastewater from treatment plants, as less water from the Jordan River entered the bay, a higher percentage of the water entering the bay was nutrient-rich, processed wastewater. The largest response was observed in phosphorus and organic carbon, both major contributors to eutrophication. While the fresh water from the Jordan River maintains low concentrations of the major cations and anions, phosphorus and organic carbon continue to be discharged into the bay from wastewater treatment facilities, allowing for blooming eutrophic conditions. While obviously not the only contributors to the environmental conditions, these three events have had the largest human-caused environmental impact in Farmington Bay.

References

- Antonielli, M., Pasqualini, S., Batini, P., Ederli, L., Massacci, A., and Loreto, F., 2002, Physiological and anatomical characterisation of *Phragmites australis* leaves: Aquatic Botany, v. 72, p. 55–66, doi:10.1016/S0304-3770(01)00220-0.
- Appleby, P.G., 2001, Chronostratigraphic Techniques in Recent Sediments, *in* Last, W.M. and Smol, J.P. eds., Tracking Environmental Change Using Lake Sediments: Basin Analysis, Coring, and Chronological Techniques, Dordrecht, Springer Netherlands, Developments in Paleoenvironmental Research, p. 171–203, doi:10.1007/0-306-47669-X_9.
- Baskin, D.K., 1997, Atomic H/C Ratio of Kerogen as an Estimate of Thermal Maturity and Organic Matter Conversion: AAPG Bulletin, v. 81, p. 1437–1450.
- Bateman, A.S., Kelly, S.D., and Jickells, T.D., 2005, Nitrogen Isotope Relationships between Crops and Fertilizer: Implications for Using Nitrogen Isotope Analysis as an Indicator of Agricultural Regime: Journal of Agricultural and Food Chemistry, v. 53, p. 5760–5765, doi:10.1021/jf050374h.
- Clark, I.D., and Fritz, P., 1997, Environmental Isotopes in Hydrogeology: Boca Raton, FL, CRC Press, 342 p.
- Clavero, E., Hernández-Mariné, M., Grimalt, J.O., and Garcia-Pichel, F., 2000, Salinity Tolerance of Diatoms from Thalassic Hypersaline Environments: Journal of Phycology, v. 36, p. 1021–1034, doi:10.1046/j.1529-8817.2000.99177.x.
- Cleverley, J.S., and Bastrakov, E.N., 2005, K2GWB: Utility for generating thermodynamic data files for The Geochemist's Workbench® at 0–1000°C and 1–5000bar from UT2K and the UNITHERM database: Computers & Geosciences, v. 31, p. 756–767, doi:10.1016/j.cageo.2005.01.007.
- Delwiche, C.C., and Steyn, P.L., 1970, Nitrogen isotope fractionation in soils and microbial reactions: Environmental Science & Technology, v. 4, p. 929–935, doi:10.1021/es60046a004.
- Dembicki, H., 2009, Three common source rock evaluation errors made by geologists during prospect or play appraisals: AAPG Bulletin, v. 93, p. 341–356, doi:10.1306/10230808076.
- Espitalie, J., Deroo, G., and Marquis, F., 1985, La pyrolyse Rock-Eval et ses applications. Deuxième partie.: Revue de l'Institut Français du Pétrole, v. 40, p. 755–784, doi:10.2516/ogst:1985045.
- France, R.L., 1995, Carbon-13 enrichment in benthic compared to planktonic algae: foodweb implications: Marine Ecology Progress Series, v. 124, p. 307–312, doi:10.3354/meps124307.
- Fry, B., 2006, Stable isotope ecology: New York, NY, Springer, 308 p.

- Fyfe, W.S., and Bischoff, J.L., 1965, The Calcite Aragonite Problem:, http://archives.datapages.com/data/sepm_sp/SP13/The_Calcite_Aragonite_Problem.htm (accessed January 2020).
- Goel, R., and Myers, L., 2009, Evaluation of Cyanotoxins in the Farmington Bay, Great Salt Lake, Utah: University of Utah, <https://pdfs.semanticscholar.org/78ed/e9c2566ad296295c7edfbab1060d298faadd.pdf>.
- Hudson, S.M., Hillam, S.A., Barker, J., Nelson, S.T., and Rey, K.A., 2019, Pyrolysis of modern wetland sediment: extracting climate records from fens in the Uinta Mountains and Fish Lake Plateau, Utah, USA: *Boreas*, v. 0, doi:10.1111/bor.12378.
- Kavanagh, L., Keohane, J., Garcia Cabellos, G., Lloyd, A., and Cleary, J., 2018, Global Lithium Sources—Industrial Use and Future in the Electric Vehicle Industry: A Review: *Resources*, v. 7, p. 57, doi:10.3390/resources7030057.
- Kim, Y.S., Choi, J.S., Kim, J.H., Kim, S.C., Park, J.W., and Kim, H.S., 2008, The effects of effluent from a closed mine and treated sewage on epilithic diatom communities in a Korean stream:, <https://www.ingentaconnect.com/content/schweiz/novh/2008/00000086/F0020003/art00009> (accessed January 2020).
- Kokke, W.C., Epstein, S., Look, S.A., Rau, G.H., Fenical, W., and Djerassi, C., 1984, On the origin of terpenes in symbiotic associations between marine invertebrates and algae (zooxanthellae). Culture studies and an application of $^{13}\text{C}/^{12}\text{C}$ isotope ratio mass spectrometry.: *Journal of Biological Chemistry*, v. 259, p. 8168–8173.
- Leavitt, P.R., Bunting, L., Moser, K., and Woodward, C., 2012, Effects of wastewater influx and hydrologic modification on algal production in the Great Salt Lake of Utah, USA - UQ eSpace: University of Regina, University of Western Ontario, <https://espace.library.uq.edu.au/view/UQ:341860> (accessed March 2019).
- Liu, X., Bo, Y., Zhang, J., and He, Y., 2015, Classification of C3 and C4 Vegetation Types Using MODIS and ETM+ Blended High Spatio-Temporal Resolution Data: *Remote Sensing*, v. 7, p. 15244–15268, doi:10.3390/rs71115244.
- Michels, A., 1998, Effects of sewage water on diatoms (Bacillariophyceae) and water quality in two tropical streams in Costa Rica: *Revista de Biología Tropical*, p. 153–175.
- Minagawa, M., and Wada, E., 1984, Stepwise enrichment of ^{15}N along food chains: Further evidence and the relation between $\delta^{15}\text{N}$ and animal age: *Geochimica et Cosmochimica Acta*, v. 48, p. 1135–1140, doi:10.1016/0016-7037(84)90204-7.
- Moser, K., Woodward, C., Leavitt, P.R., and Wurtsbaugh, W.A., 2012, Historical Changes in Aquatic Invertebrates and Charophytes of the Great Salt Lake, Utah (USA): The Effects of Wastewater Inputs, Water Diversions and Barriers: University of Western Ontario.

- Myrbo, A., Morrison, A., and McEwan, R., 2011, TMI - Smear Slides - Home: Tool for Microscopic Identification, <https://tmi.lacore.umn.edu/> (accessed April 2019).
- Nable, R.O., Bañuelos, G.S., and Paull, J.G., 1997, Boron toxicity: Plant and Soil, v. 193, p. 181–198, doi:10.1023/A:1004272227886.
- Naftz, D., Angerth, C., Kenney, T., Waddell, B., Darnall, N., Silva, S., Perschon, C., and Whitehead, J., 2008, Anthropogenic influences on the input and biogeochemical cycling of nutrients and mercury in Great Salt Lake, Utah, USA: Applied Geochemistry, v. 23, p. 1731–1744, doi:10.1016/j.apgeochem.2008.03.002.
- Naftz, D.L., Stephens, D.W., Callender, E., and Van Metre, P.C., 2000, Reconstructing historical changes in the environmental health of watersheds by using sediment cores from lakes and reservoirs in Salt Lake Valley, Utah: US Geol. Surv. Fact Sheet FS-164-00,.
- National Lacustrine Core Facility (LacCore) : University of Minnesota, <http://lrc.geo.umn.edu/lacore/> (accessed February 2020).
- Ogino, T., Suzuki, T., and Sawada, K., 1987, The formation and transformation mechanism of calcium carbonate in water: Geochimica et Cosmochimica Acta, v. 51, p. 2757–2767, doi:10.1016/0016-7037(87)90155-4.
- Peters, K.E., 1986, Guidelines for Evaluating Petroleum Source Rock Using Programmed Pyrolysis: AAPG Bulletin, v. 70, p. 318–329.
- Saltonstall, K., Burdick, D., Miller, S., and Smith, B., 2005, Native and Non-native Phragmites: Challenges in Identification, Research, and Management of the Common Reed: National Estuarine Research Reserve Technical Report Series,.
- Schnurrenberger, D., Russell, J., and Kelts, K., 2003, Classification of lacustrine sediments based on sedimentary components: Journal of Paleolimnology, v. 29, p. 141–154, doi:10.1023/A:1023270324800.
- Strack, D., 2019, Salt Lake Meat Packing: UtahRails.net, <http://utahrails.net/industries/meat-packing-salt-lake.php> (accessed January 2020).
- Verardo, D.J., Froelich, P.N., and McIntyre, A., 1990, Determination of organic carbon and nitrogen in marine sediments using the Carlo Erba NA-1500 analyzer: Deep Sea Research Part A. Oceanographic Research Papers, v. 37, p. 157–165, doi:10.1016/0198-0149(90)90034-S.
- Wada, E., Kadonaga, T., and Matsuo, S., 1975, ^{15}N abundance in nitrogen of naturally occurring substances and global assessment of denitrification from isotopic viewpoint: GEOCHEMICAL JOURNAL, v. 9, p. 139–148, doi:10.2343/geochemj.9.139.
- Whittaker, M., Pollard, S.J.T., Fallick, A.E., and Preston, T., 1996, Characterisation of refractory wastes at hydrocarbon-contaminated sites—II. Screening of reference oils by stable

carbon isotope fingerprinting: *Environmental Pollution*, v. 94, p. 195–203,
doi:10.1016/S0269-7491(96)00062-0.

Wray, J.L., and Daniels, F., 1957, Precipitation of Calcite and Aragonite: *Journal of the American Chemical Society*, v. 79, p. 2031–2034, doi:10.1021/ja01566a001.

Wurtsbaugh, W., 2012, Paleolimnological Analysis of the History of Metals Contamination in the Great Salt Lake, Utah: 1Final report from Utah State University, University of Regina and University of Western Ontario to Utah State Department of Environmental Quality, p. 1–42.

Wurtsbaugh, W., and Marcarelli, A., 2006, Eutrophication in Farmington Bay, Great Salt Lake, Utah 2005 Annual Report: Utah State University,
https://digitalcommons.usu.edu/cgi/viewcontent.cgi?article=1559&context=wats_facpub.

Wurtsbaugh, W., Marcarelli, A., Christison, C., Moore, J., Gross, D., Bates, S., and Kircher, S., 2002, Comparative Analysis of Pollution in Farmington Bay and the Great Salt Lake, Utah: A Report to the Utah Division of Water Quality, p. 21.



Figure 1. Location from where both freeze cores were obtained from Farmington Bay.



Figure 2. Image of the freeze core just after being removed from the bay. Laminations are clearly visible, illustrating the fact that disruption is limited by using this coring method.

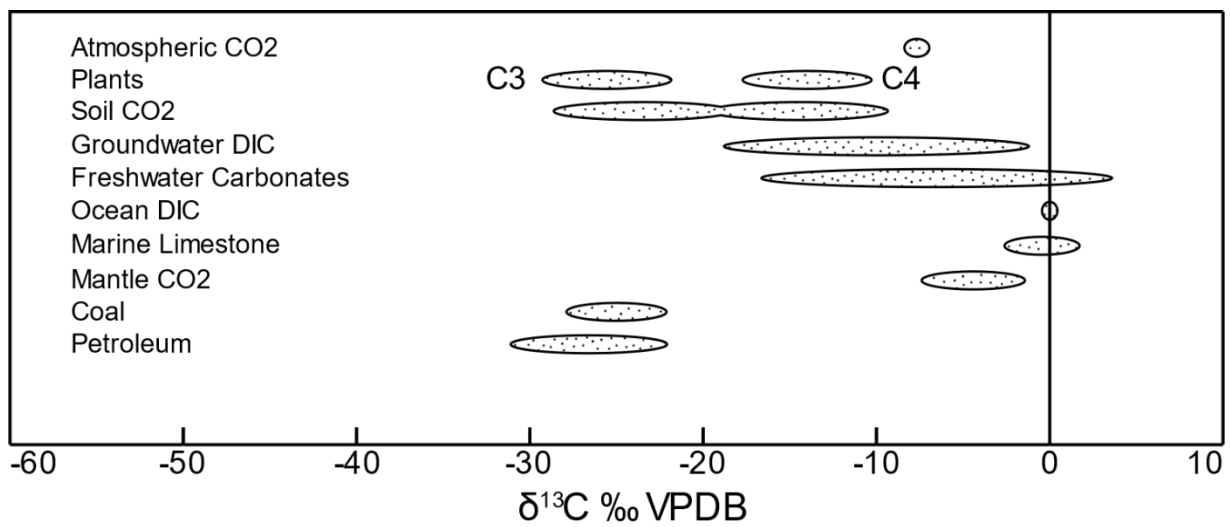
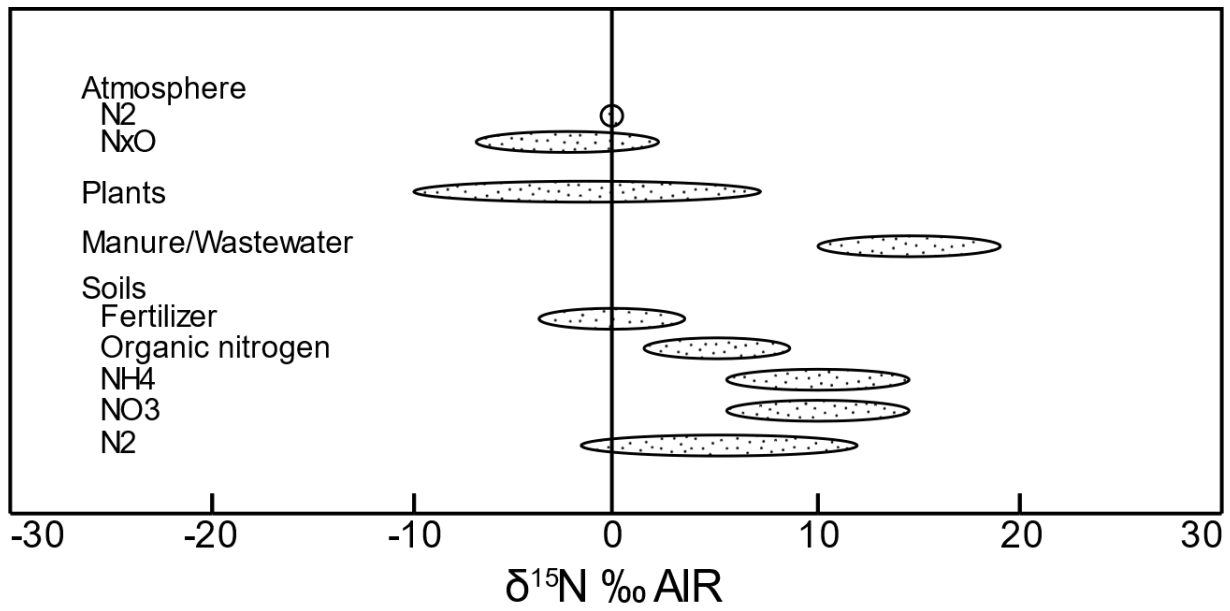


Figure 4. Changes in major nutrient sources illustrated based on their $\delta^{15}\text{N}$ value with respect to atmospheric nitrogen (top) and $\delta^{13}\text{C}$ values with respect to VPDB (bottom). Adapted from Clark and Fritz (1997).

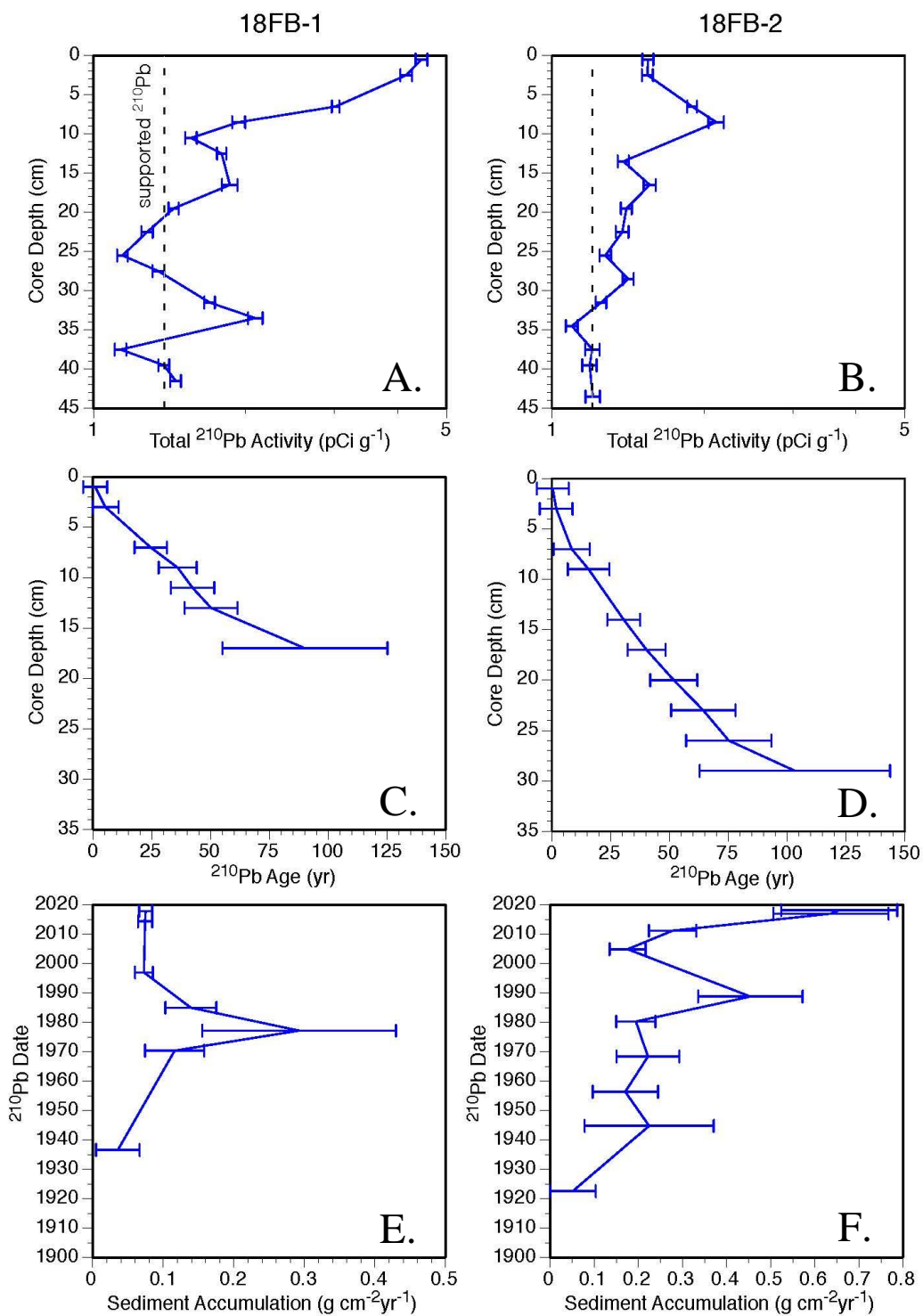


Figure 5. ^{210}Pb data showing calculated ages and sedimentation rates of both FB-1 and FB-2 based on the CRS model.

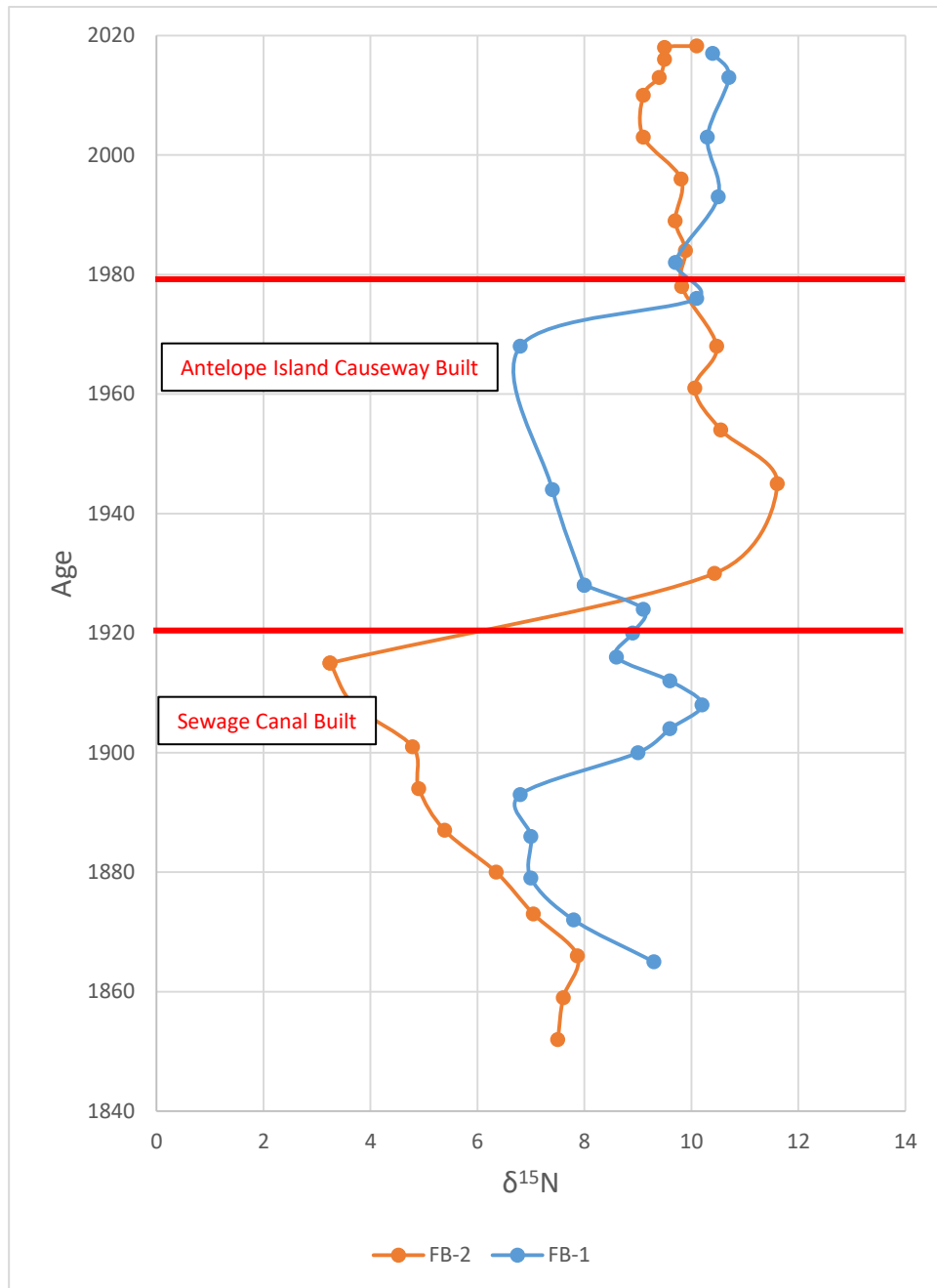


Figure 6. Isotope data for both cores that shows the enrichment in $\delta^{15}\text{N}$ values with respect to time.

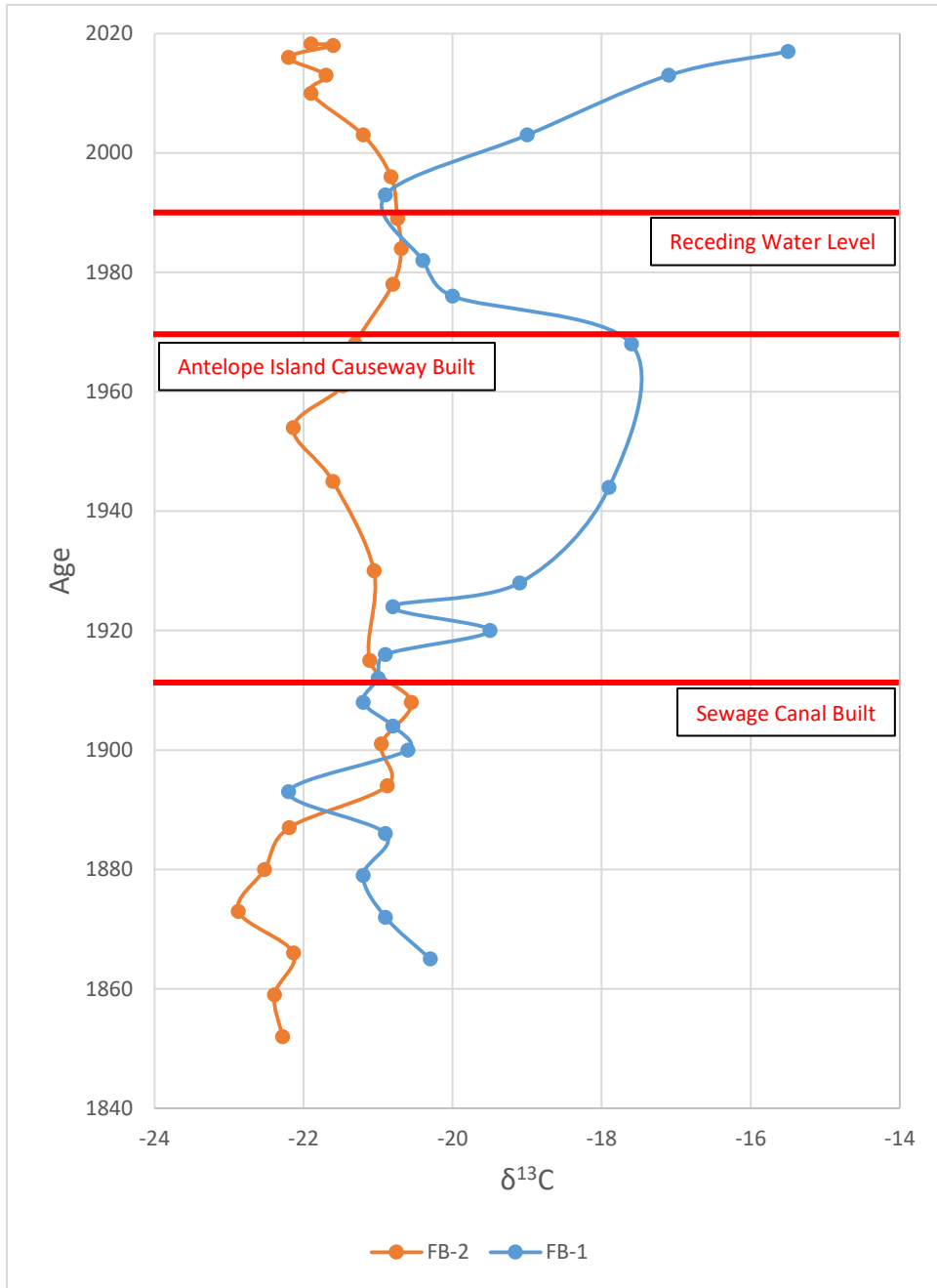


Figure 7. $\delta^{13}\text{C}$ isotope data for both cores illustrating a relatively constant value for FB-2 and an enrichment in FB-1.

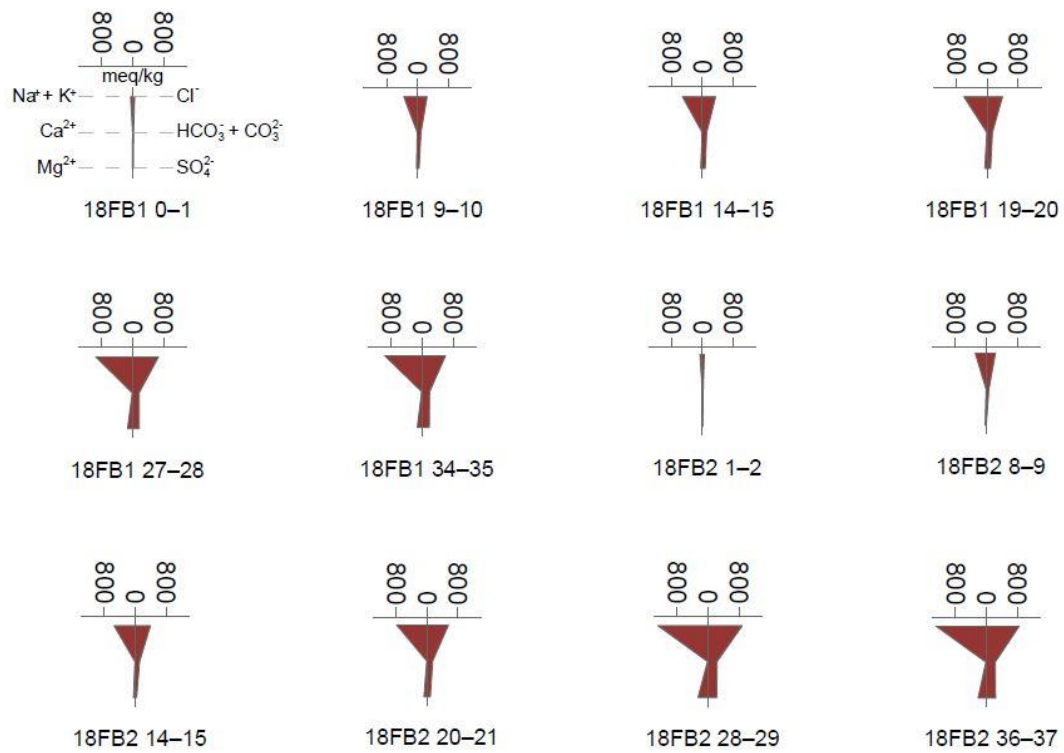


Figure 8. Stiff diagrams from select depths of both cores illustrate the freshening effect in the bay as the major cations and anions decrease from bottom to top.

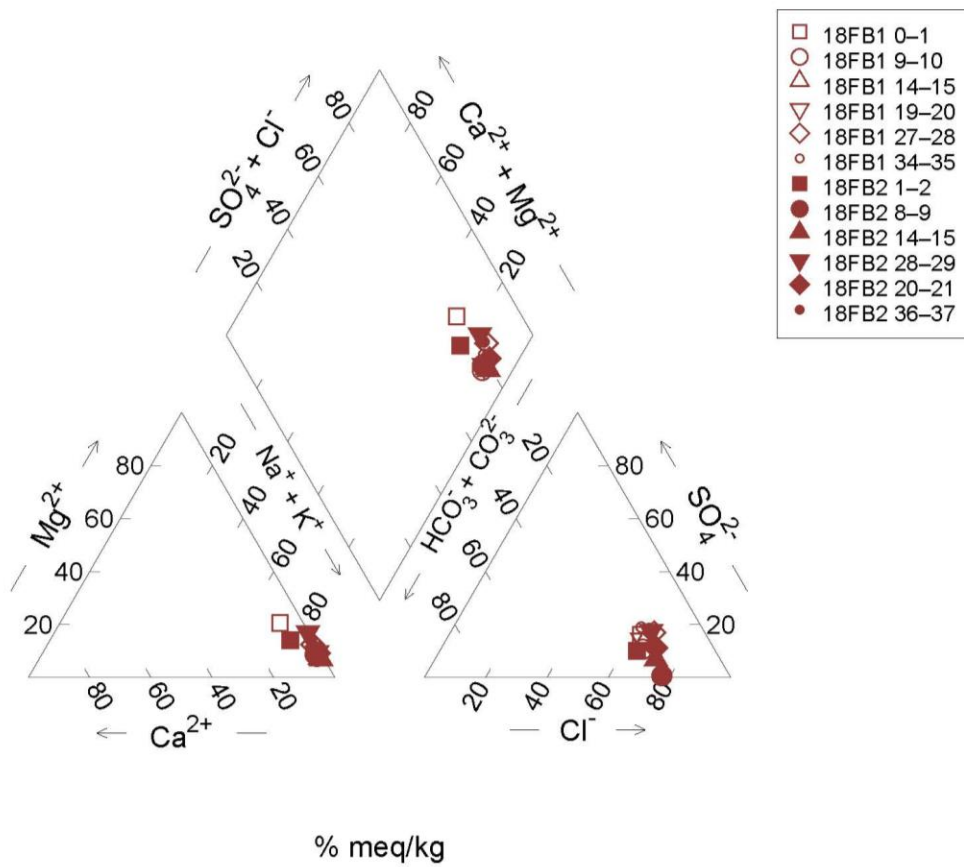


Figure 9. Samples plot on top of each other on the Piper diagram indicating that the cations and anions are all decreasing at relatively the same rate.

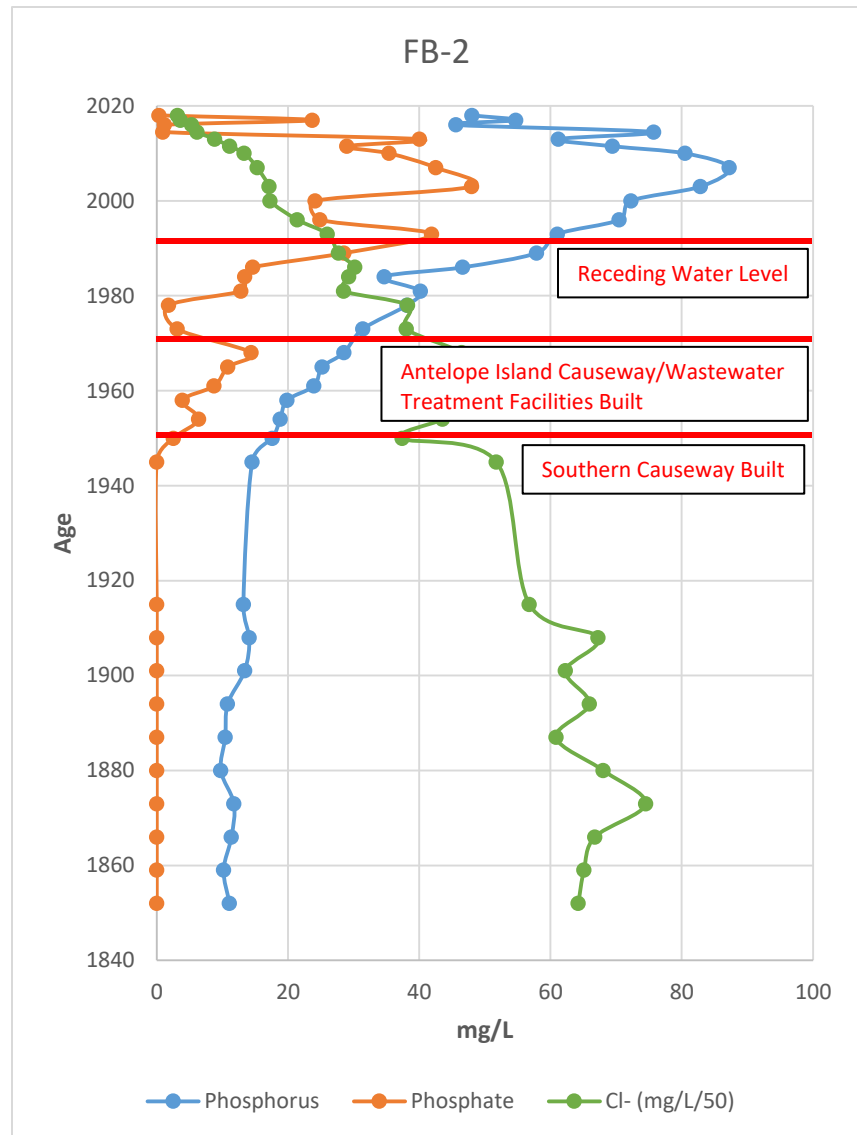
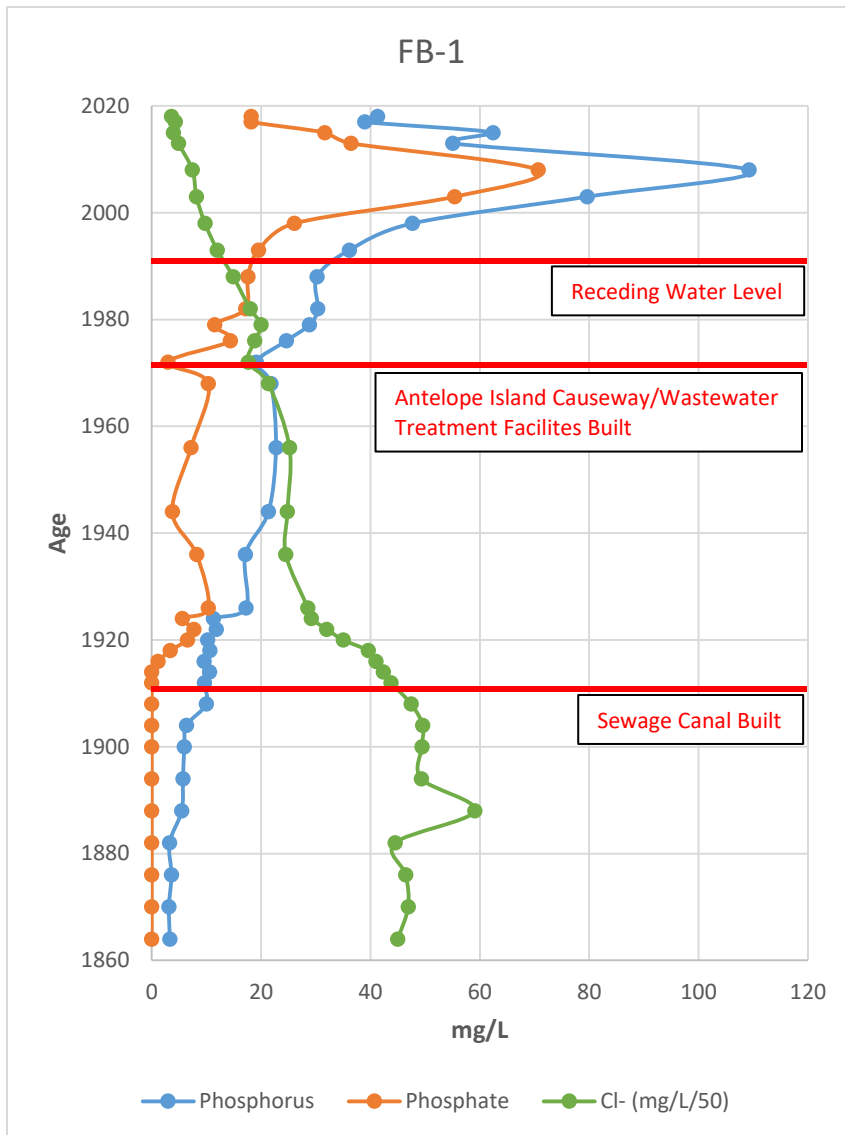


Figure 10. Phosphorus results from both ICP and IC analysis with conservative tracer Cl⁻. The increase in concentration in FB-1 corresponds to the completion of the sewage canal while the concentrations in FB-2 do not begin to increase until the 1950's. A dramatic increase is observed in both cores beginning around 1990.

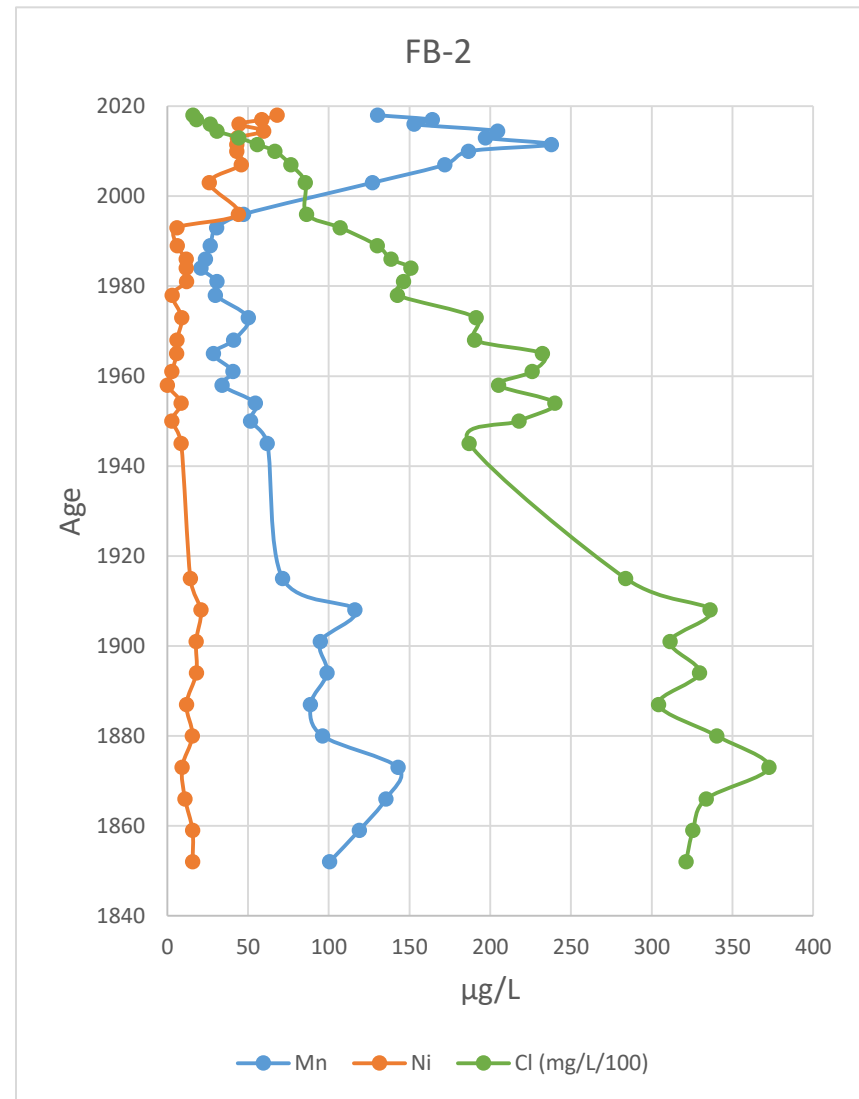
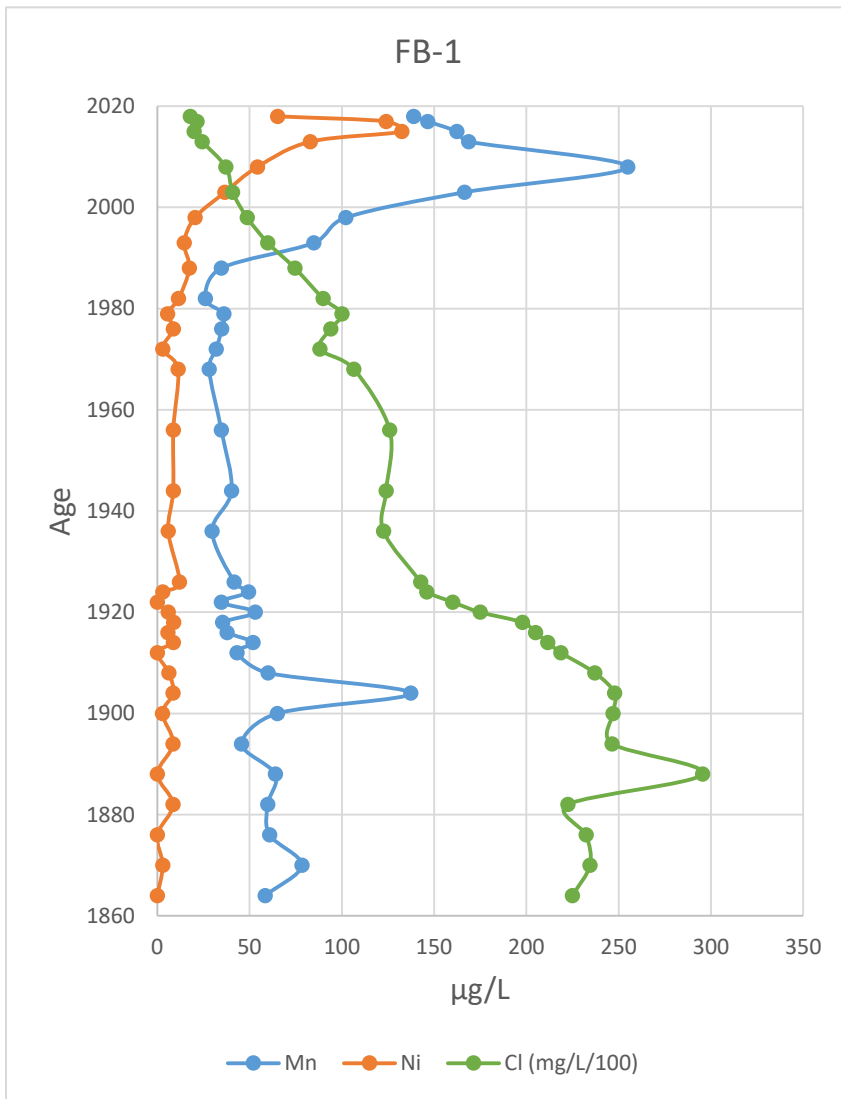


Figure 11. Trace metals Mn and Ni plotted with conservative tracer Cl. Both cores show little variation in concentrations of the metals, but increase beginning around 1990.

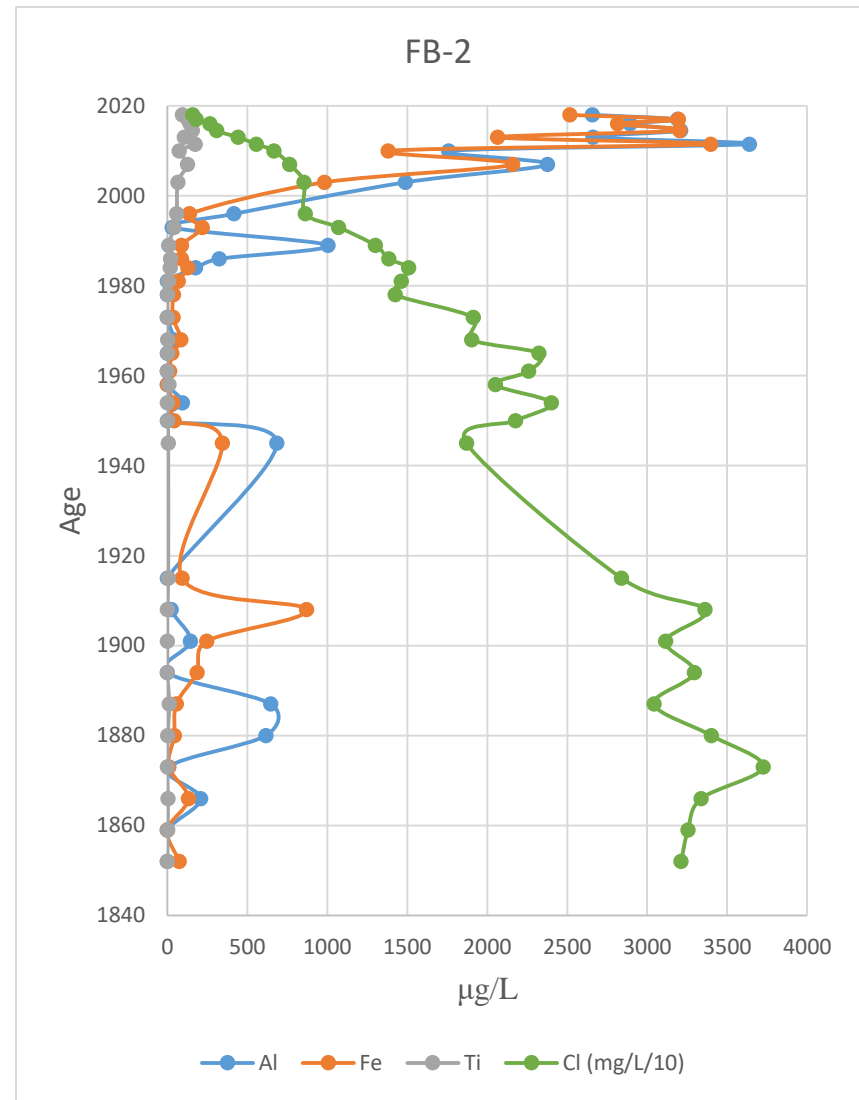
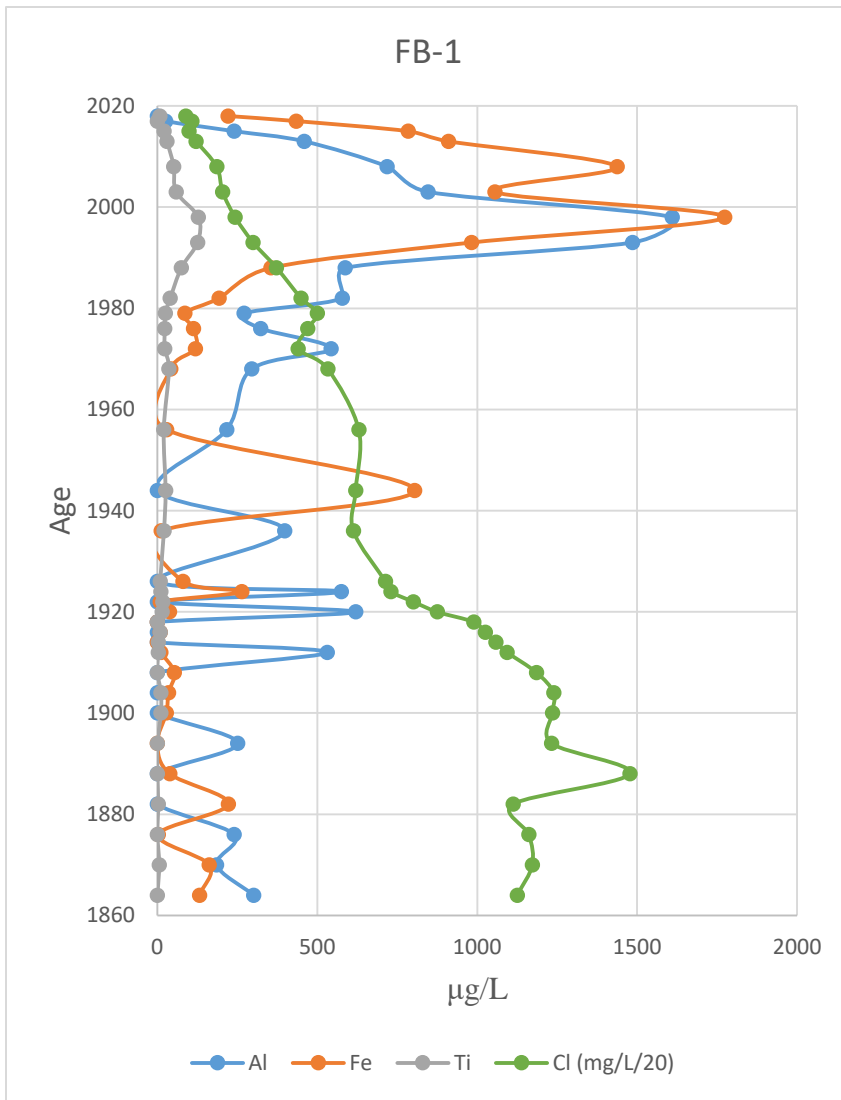


Figure 12. Trace metals Al, Fe and Ti plotted with conservative tracer Cl^- . In FB-1 an increase in concentration followed by a decrease is observed near the top of FB-1 while all 3 continuously increase at the top of FB-2.

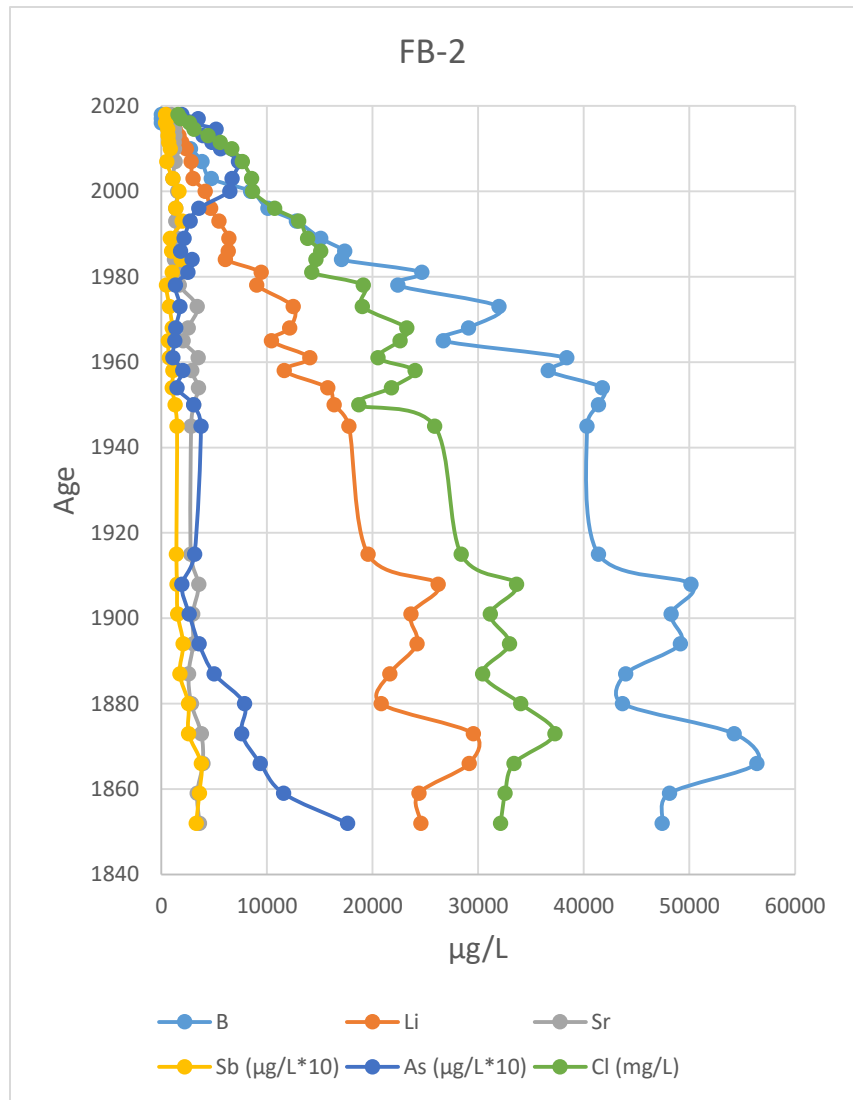
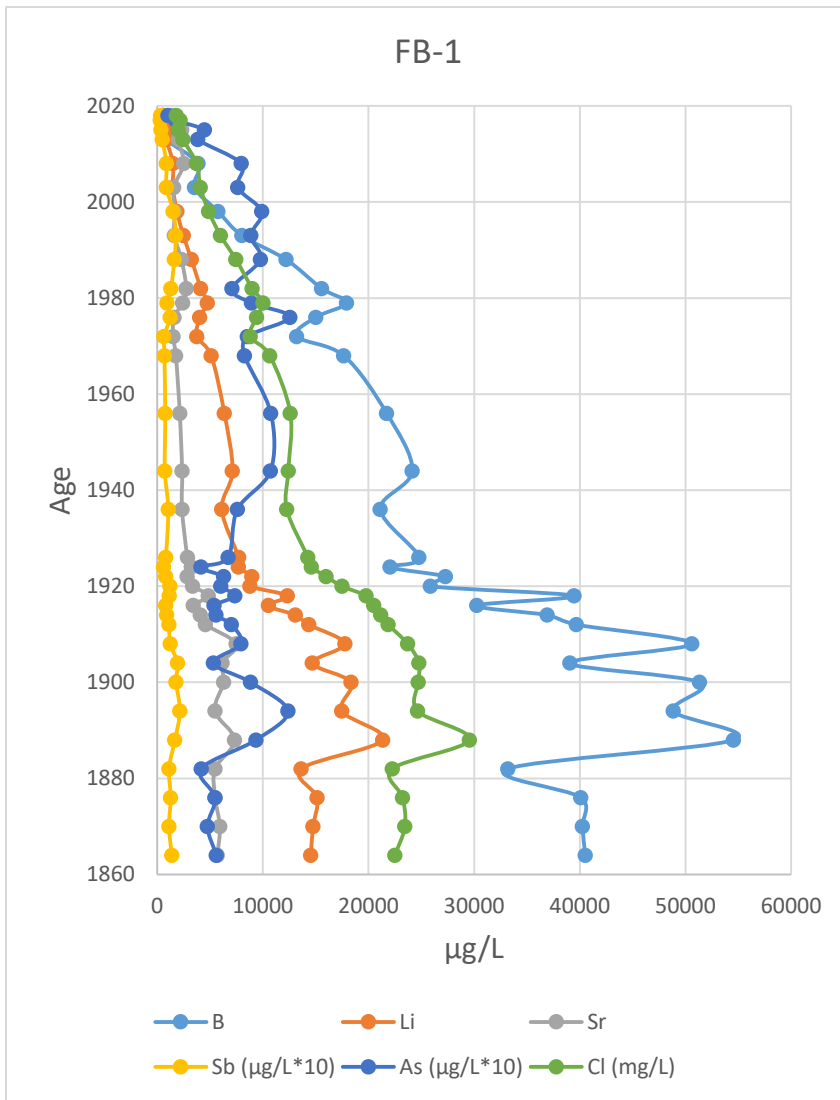


Figure 13. Trace metals B, Li, Sr, Sb, and As plotted with conservative tracer Cl. Both cores exhibit a large decrease in concentrations for all these trace metals from the bottom to the top of the core.

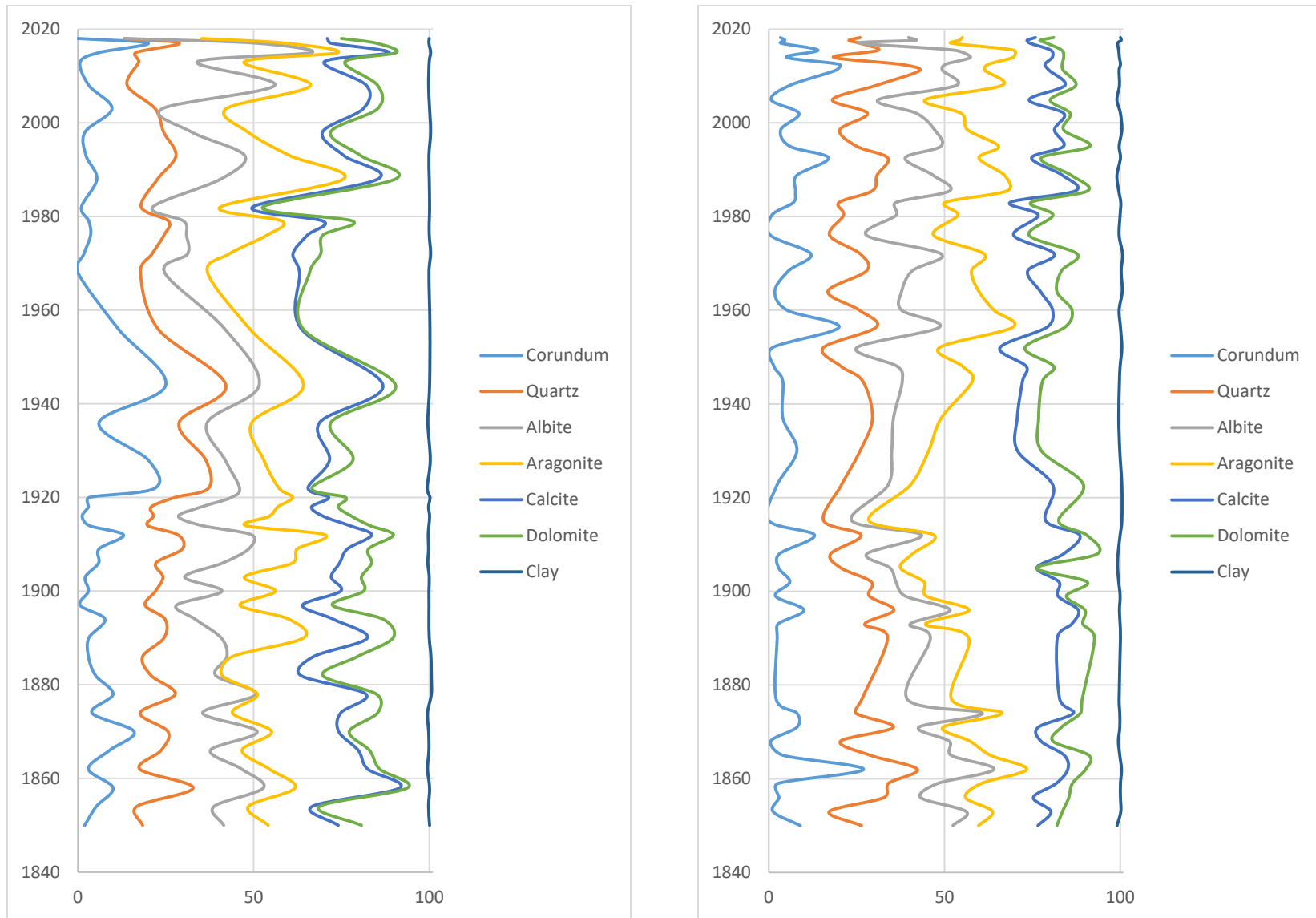


Figure 14. Composite mineralogy results for FB-1 (left) and FB-2 (right) from Rietveld analysis.

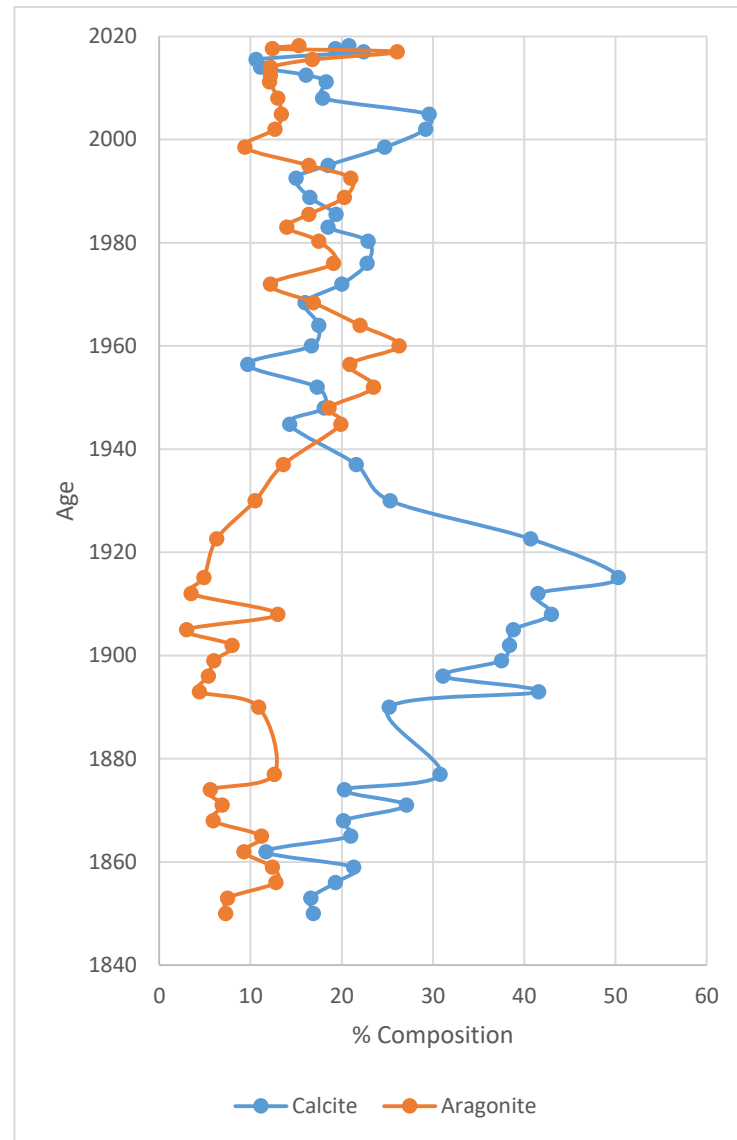
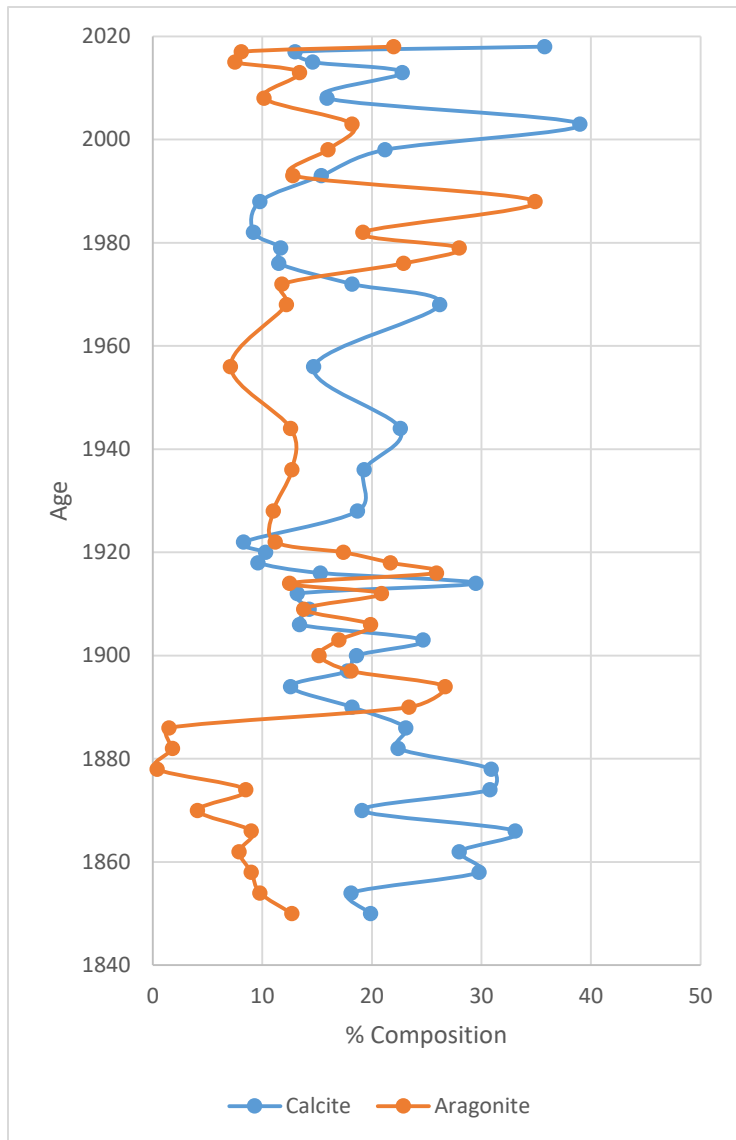


Figure 15. Calcite and aragonite variations shown in FB-1 (left) and FB-2 (right). Both show a pattern of decreasing calcite and increasing aragonite beginning in the early 1900's.

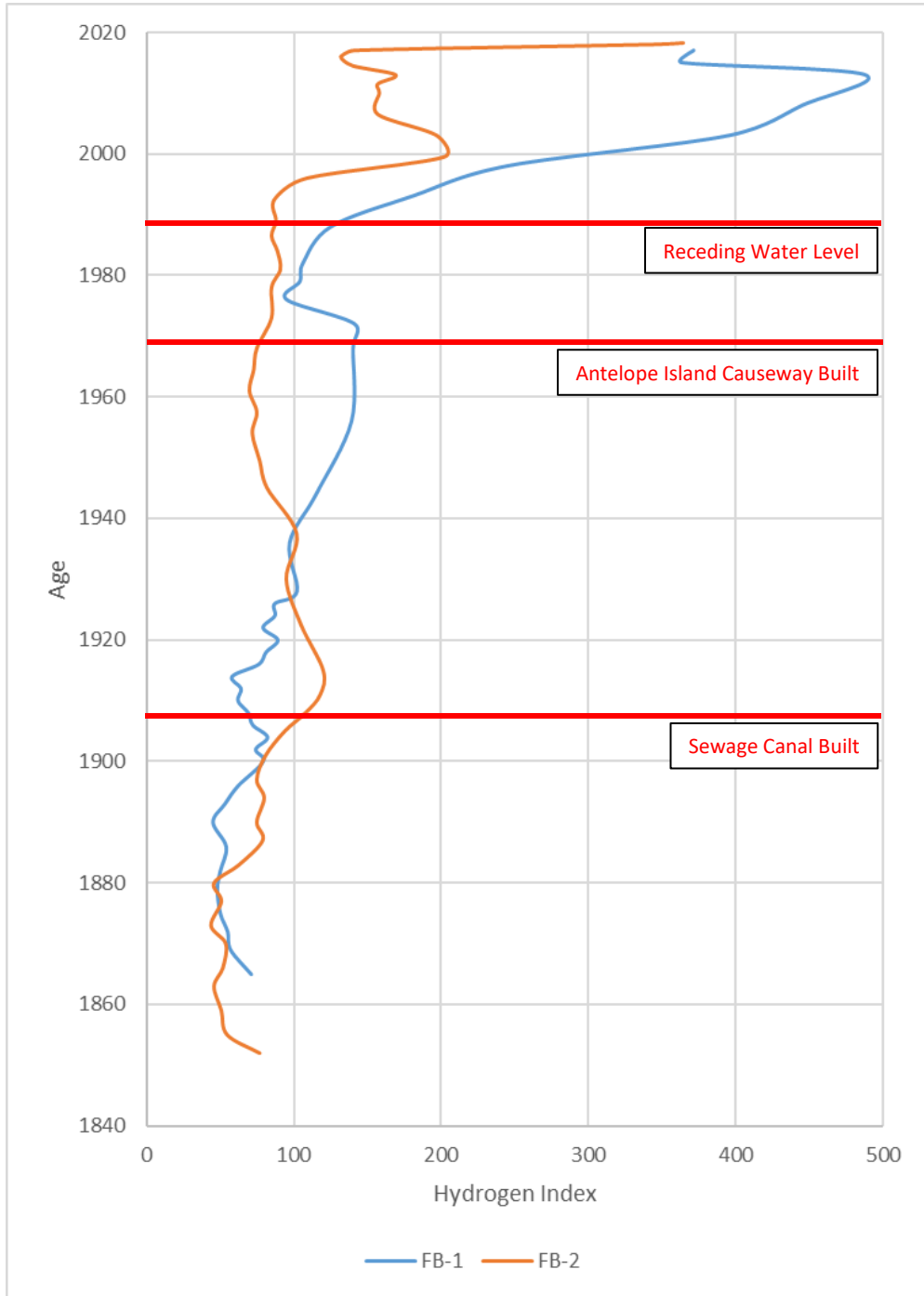


Figure 16. HI values from Rock-Eval Pyrolysis for both FB-1 and FB-2 exhibiting a sudden increase near the surface of the cores.

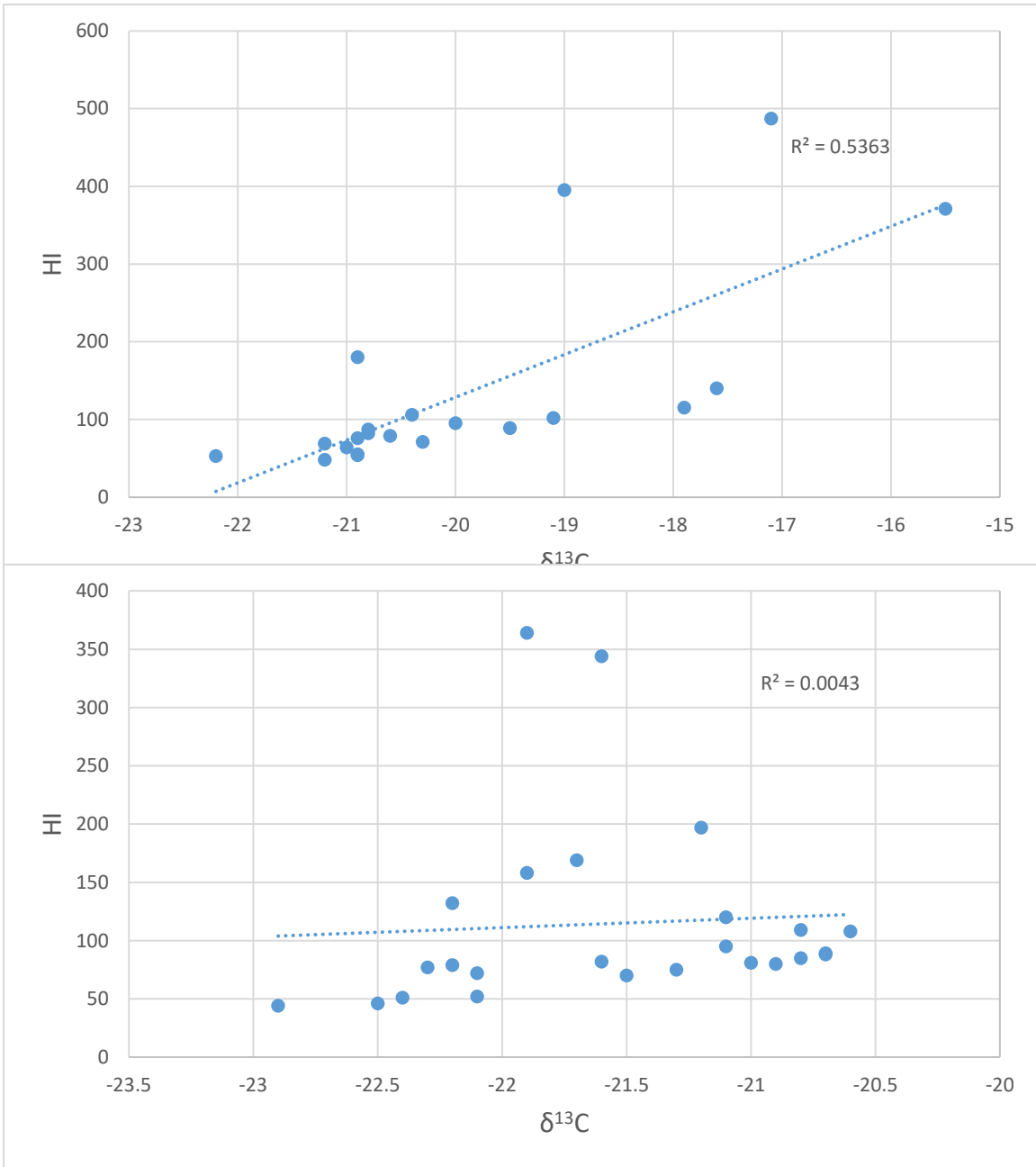


Figure 17. Strong correlation between the hydrogen index and $\delta^{13}C$ exhibited in FB-1 (top) while no correlation is seen in FB-2 (bottom) which is likely a result of the inflow of fresh water from the Jordan River.

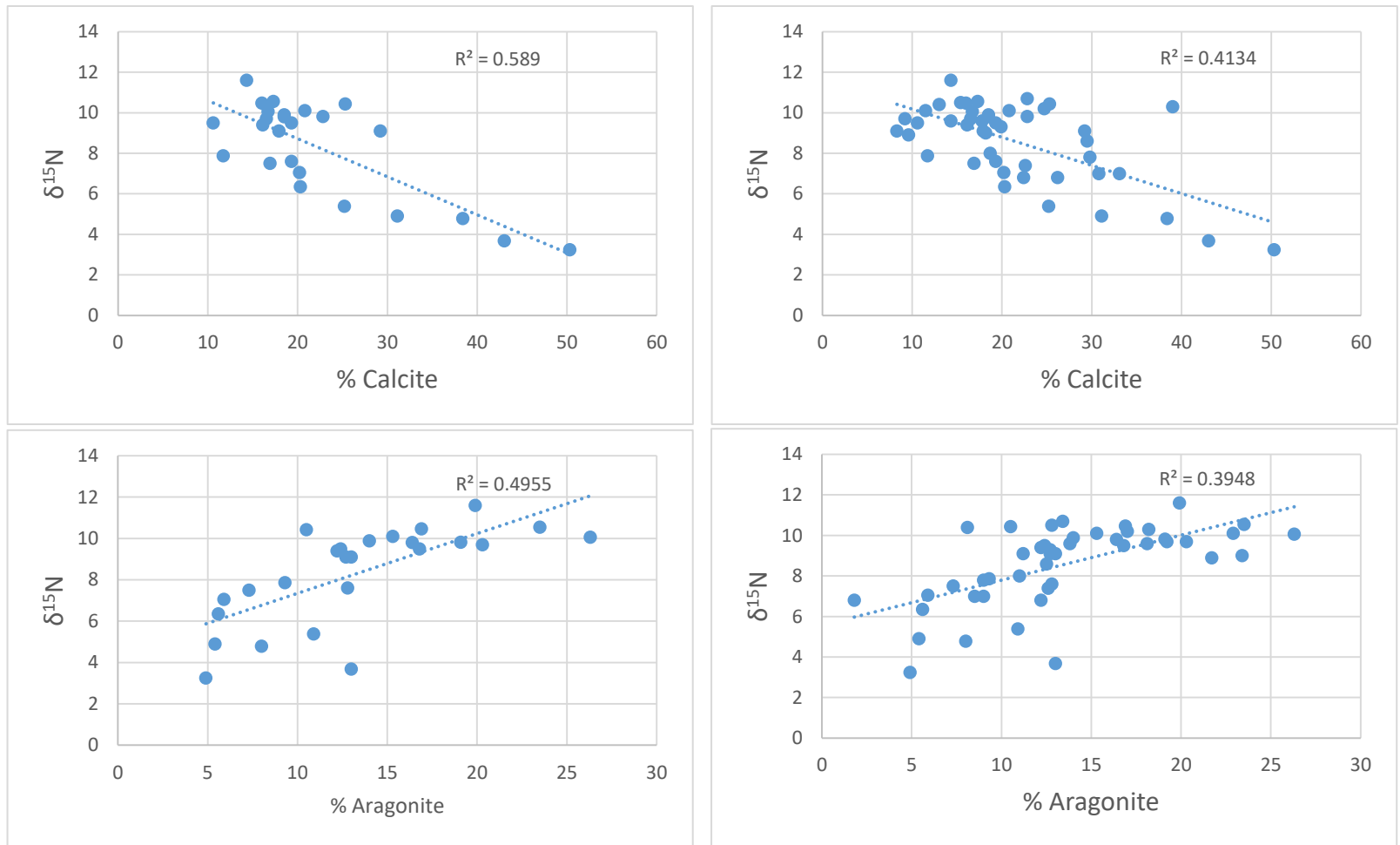


Figure 18. Correlation between $\delta^{15}\text{N}$ and calcite and aragonite composition. Results for data from FB-2 is shown in figures A and B while figures C and D represent the data from both cores.

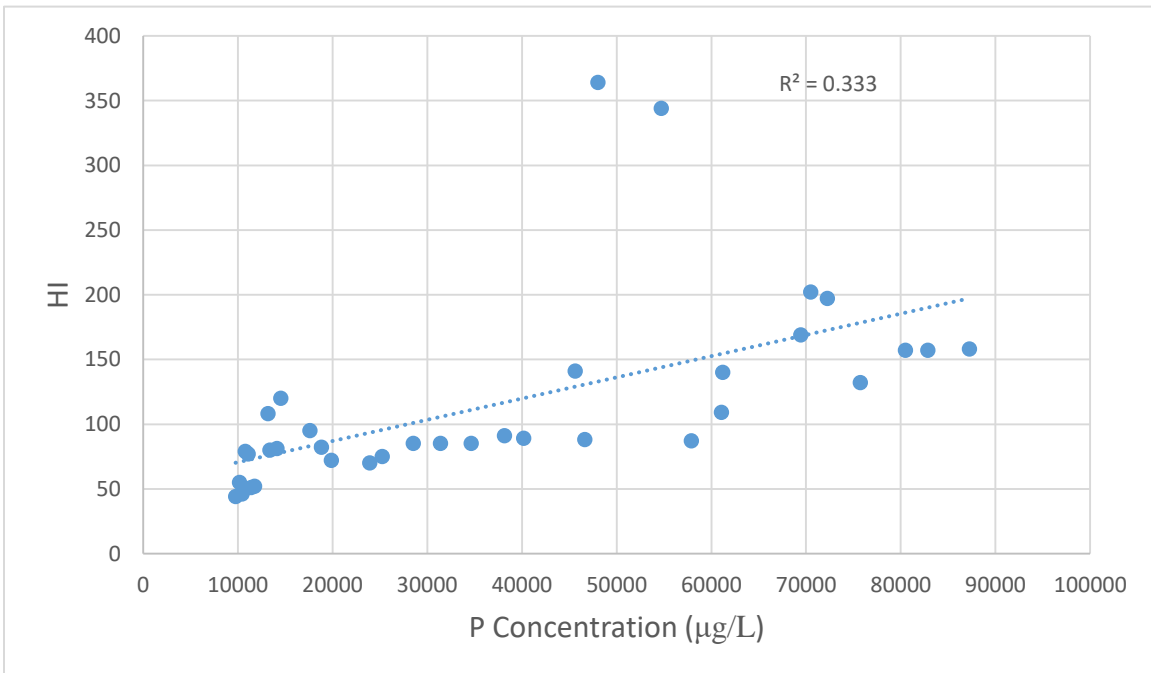
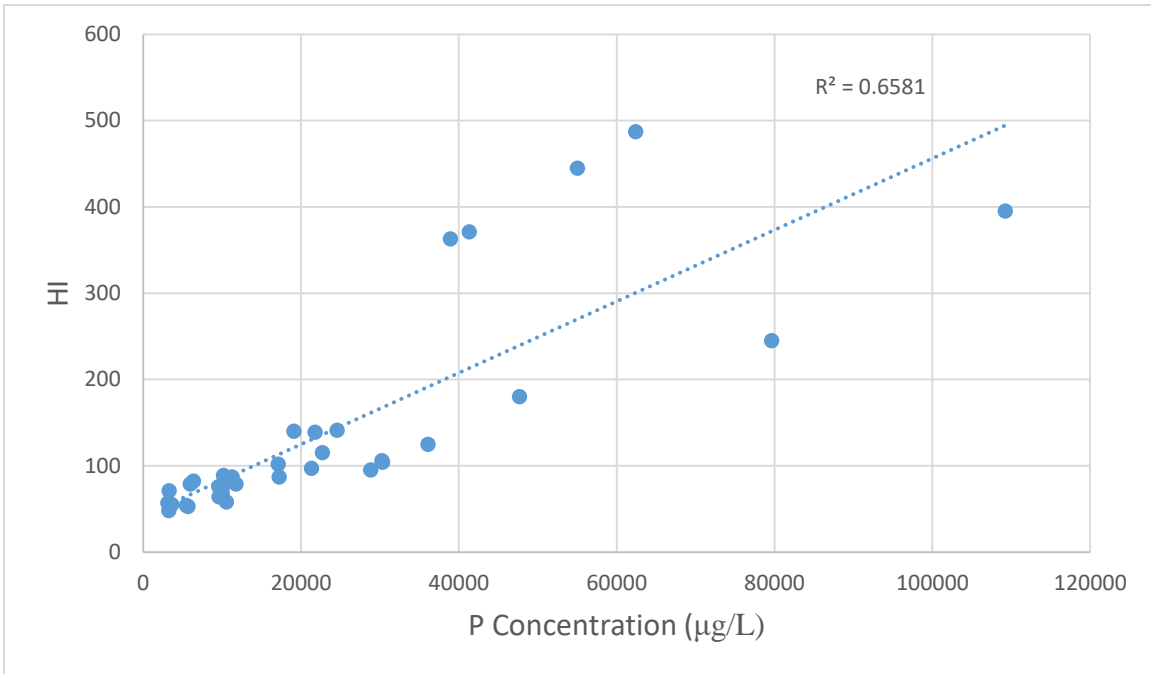
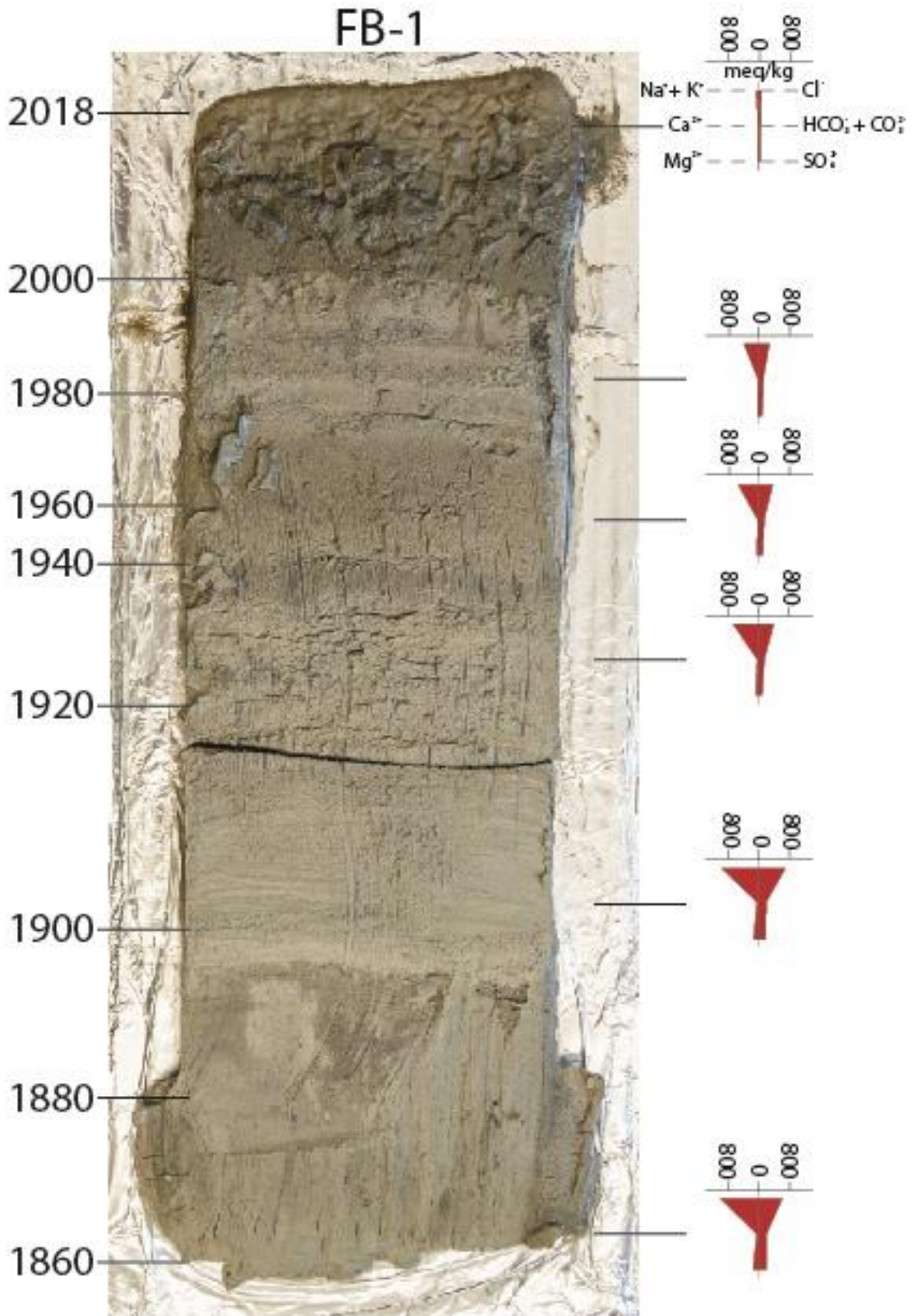
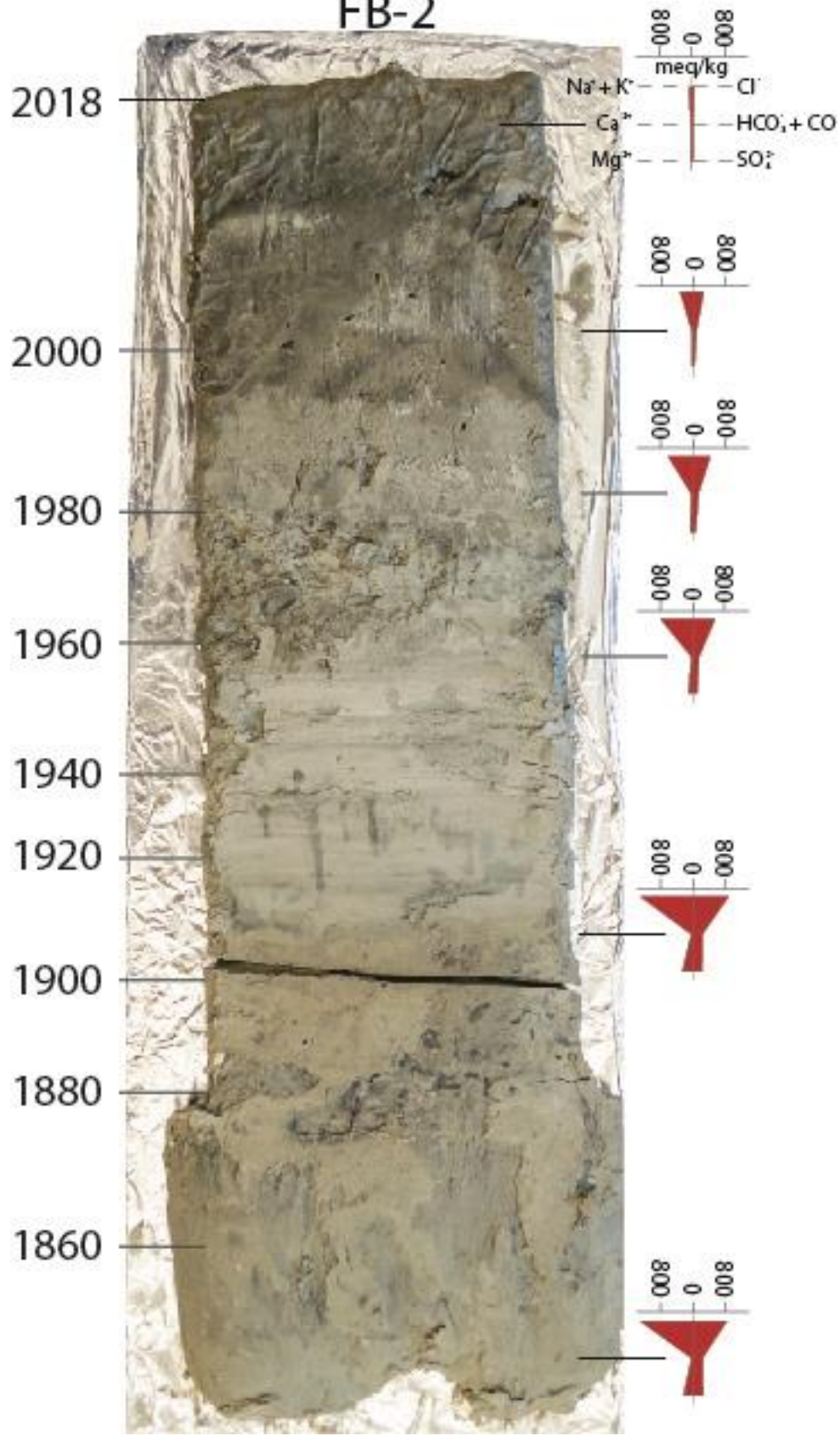


Figure 19. Correlation between the hydrogen index and phosphorus concentration shown to be strong in FB-1 (top) though not as strong in FB-2 (bottom) which is likely a result of the inflow of fresh water from the Jordan River.

Appendix A

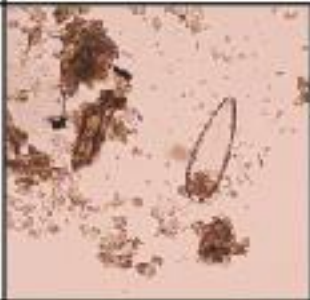
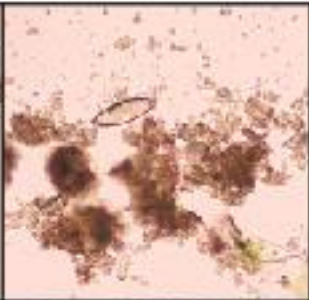
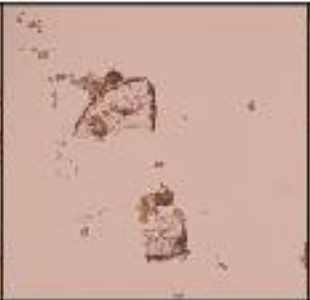
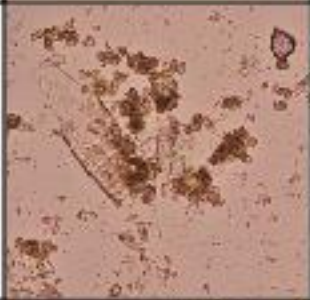
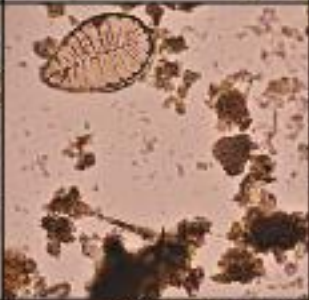
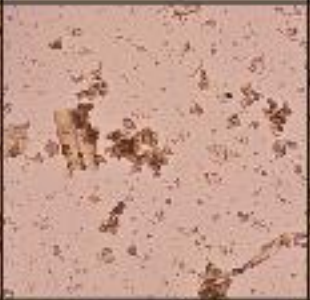
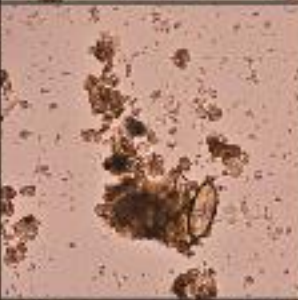
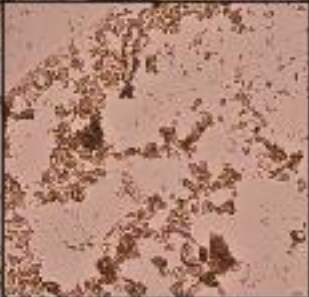
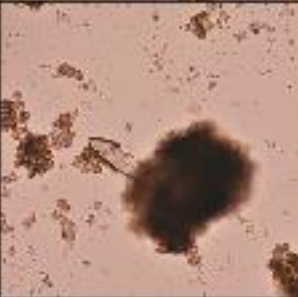


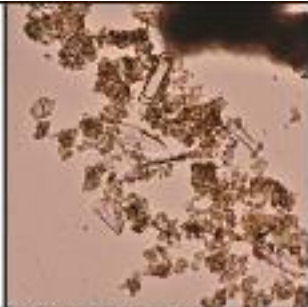
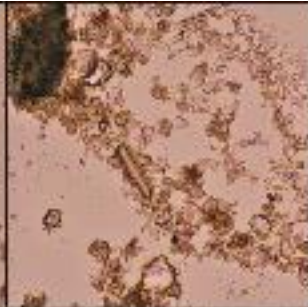
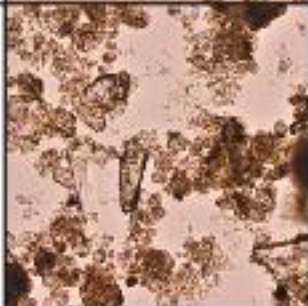
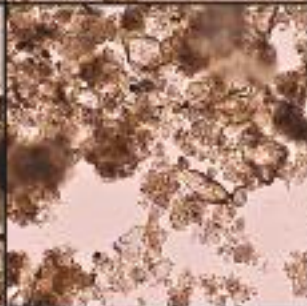
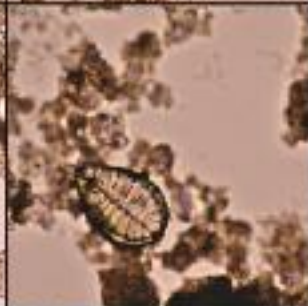
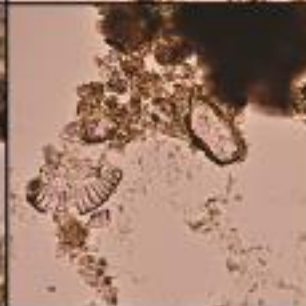
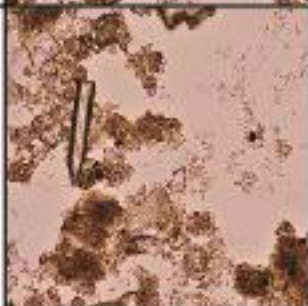
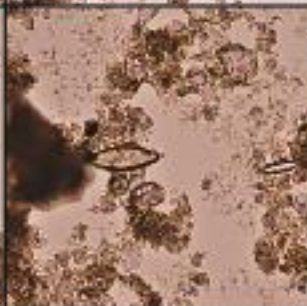
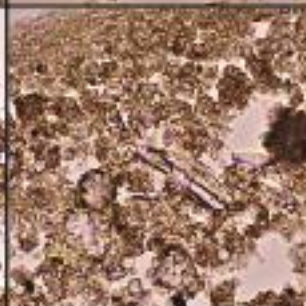
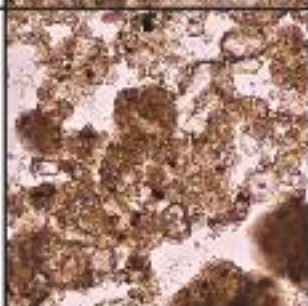
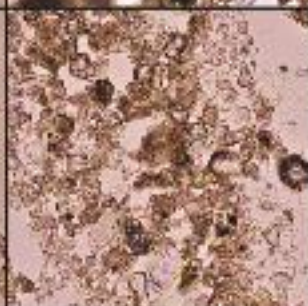
FB-2

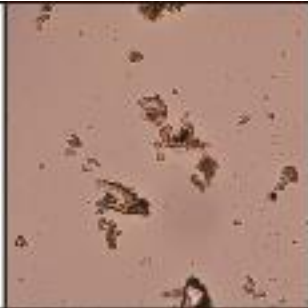
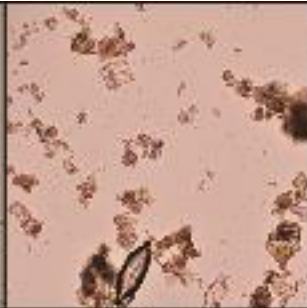
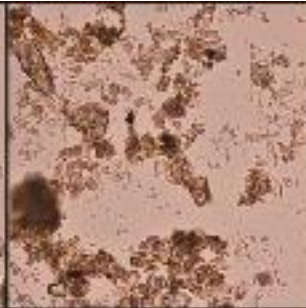
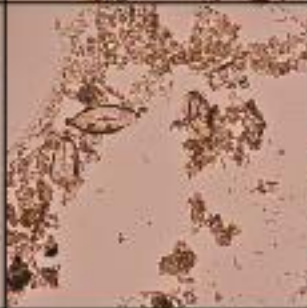
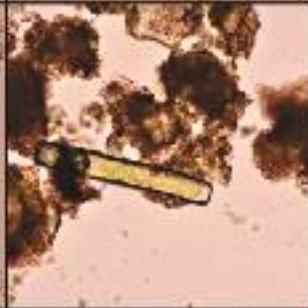
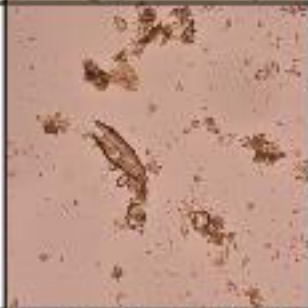
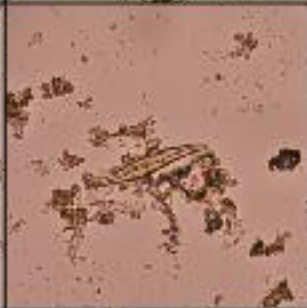
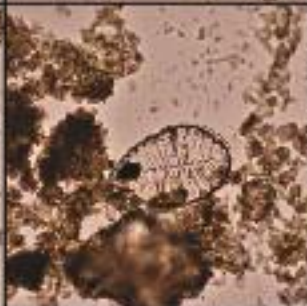
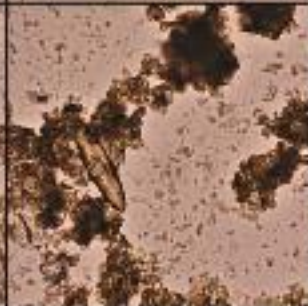
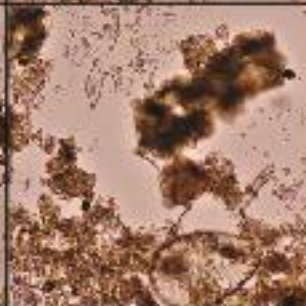


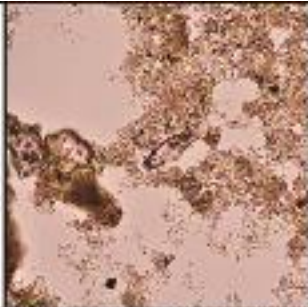
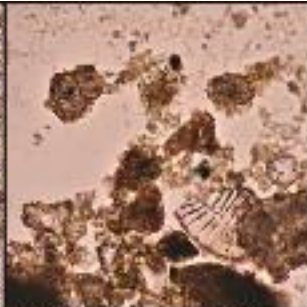
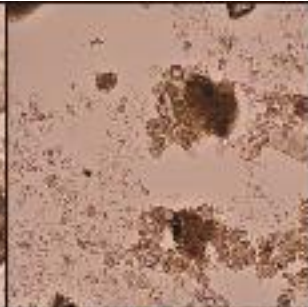
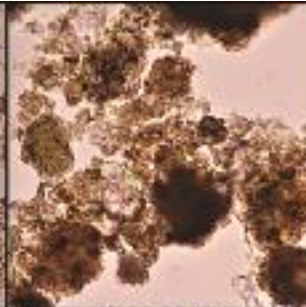
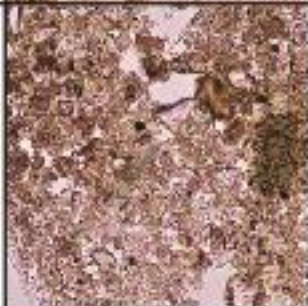
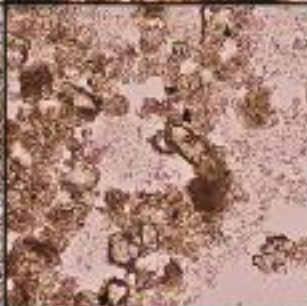
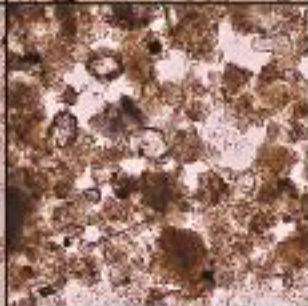
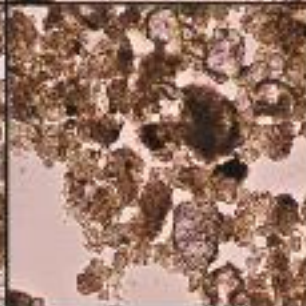
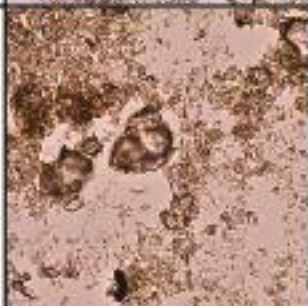
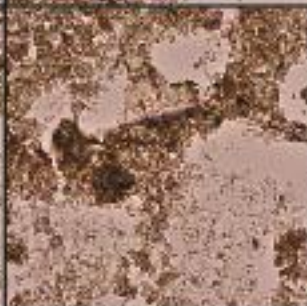
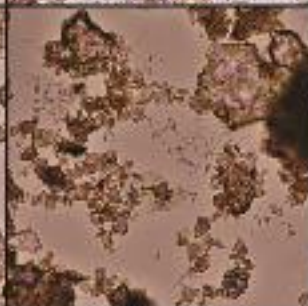
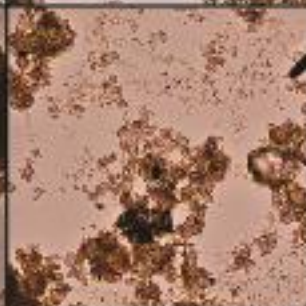
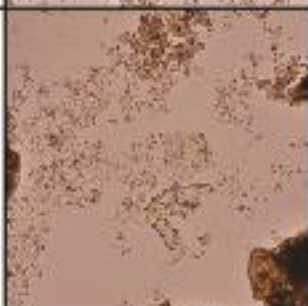
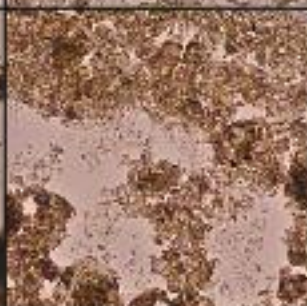
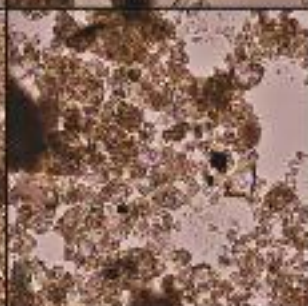
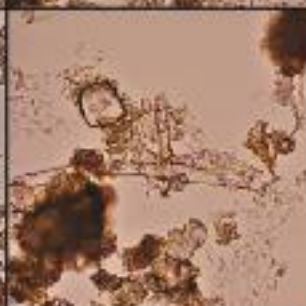
Appendix B

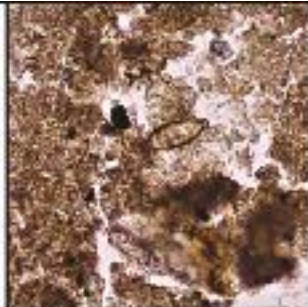
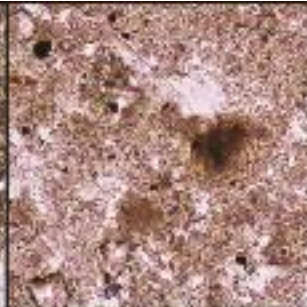
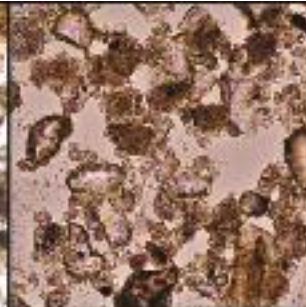
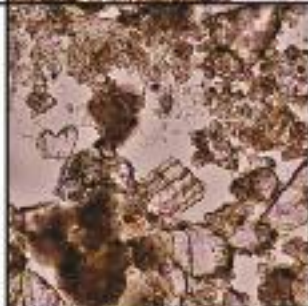
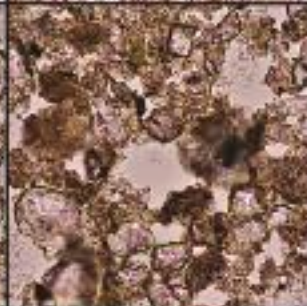
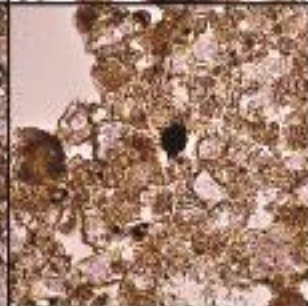
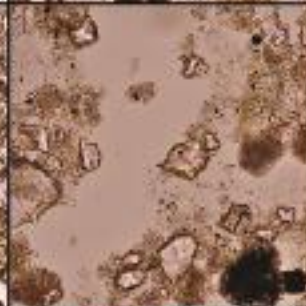
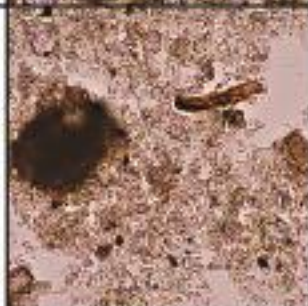
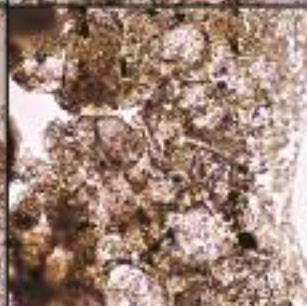
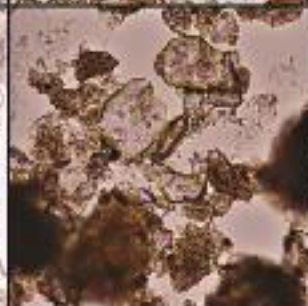
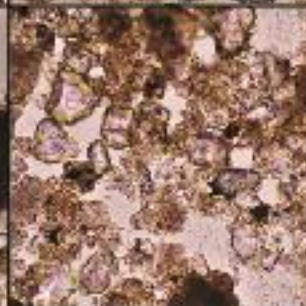
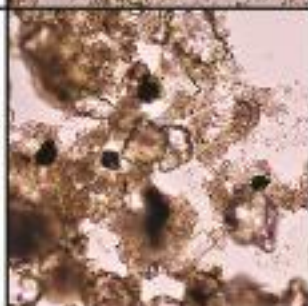
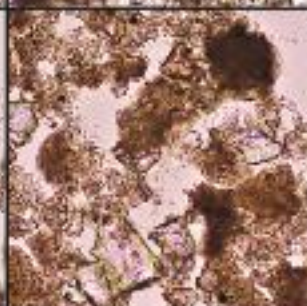
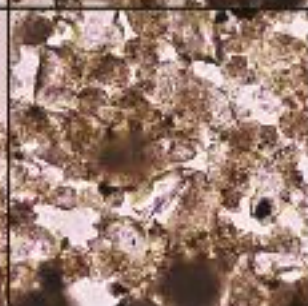
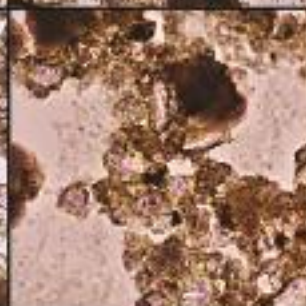
FB-1

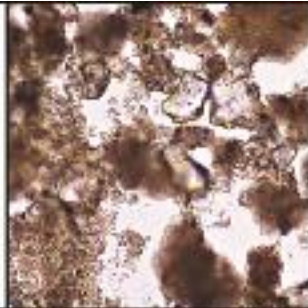
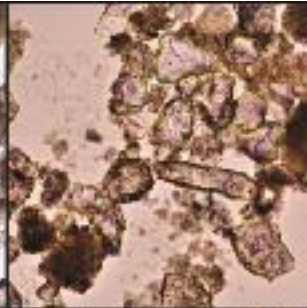
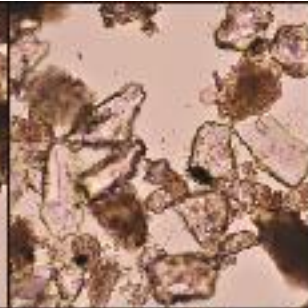
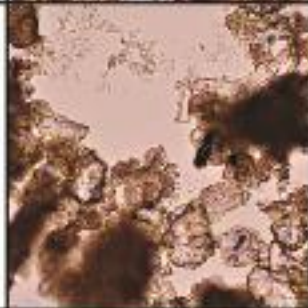
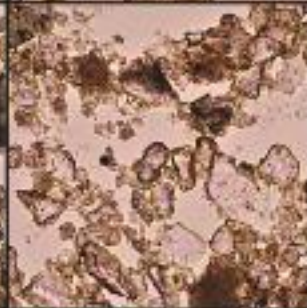
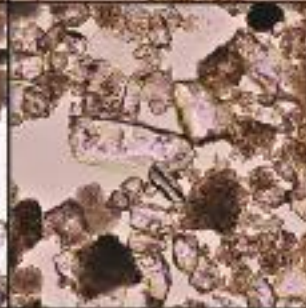
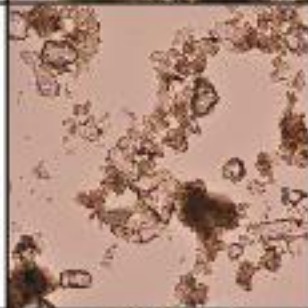
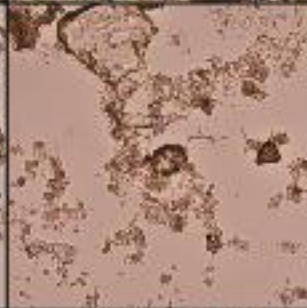
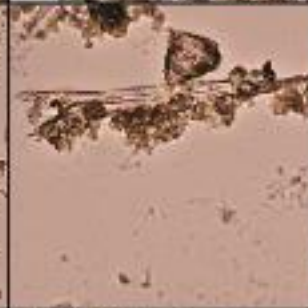
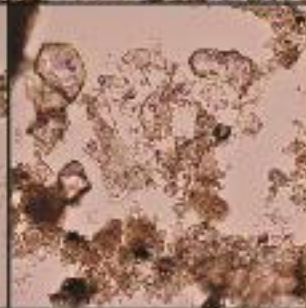
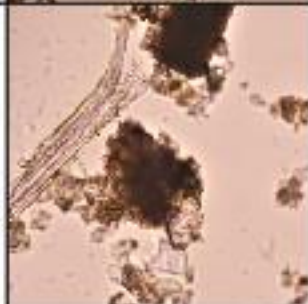
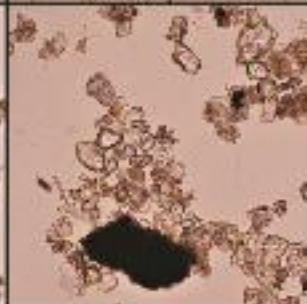
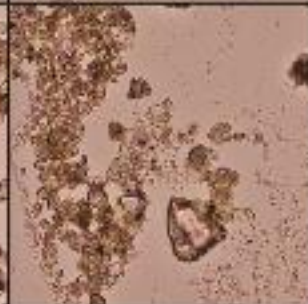
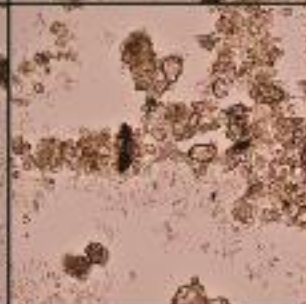
Depth	Description	Images			
0-1 cm	Mostly inorganic material; high number of diatoms; some plant and algal material				
1-2 cm	Mostly inorganic material; high number of diatoms; some plant and algal material				
2-3 cm	Mostly inorganic material; high number of diatoms; some plant and algal material				

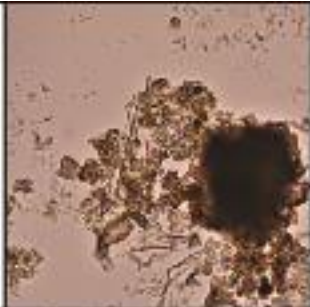
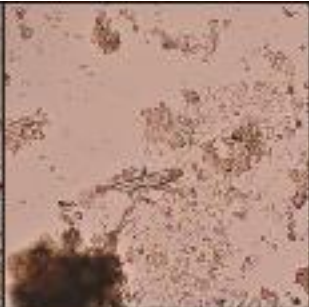
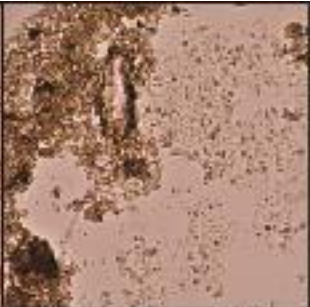
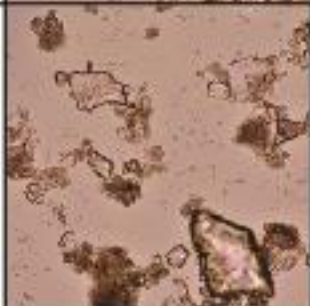
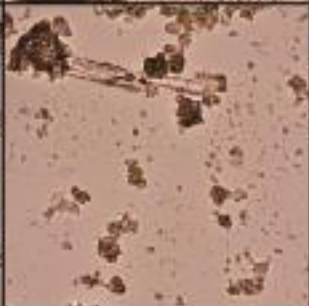
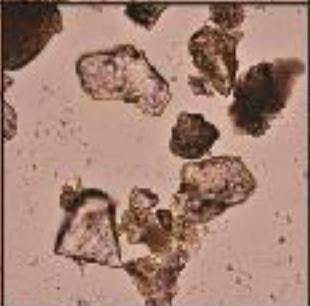
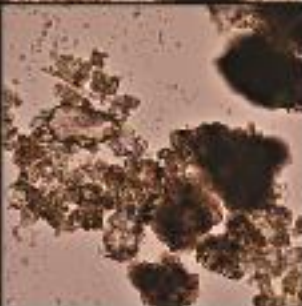
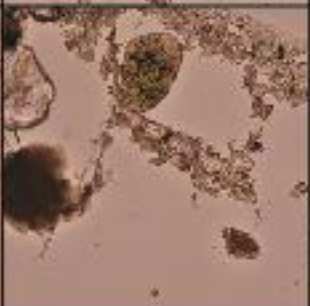
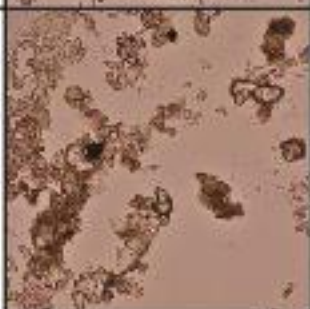
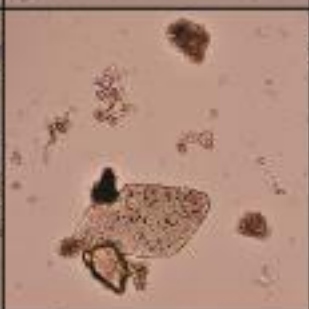
7-8 cm	Mostly inorganic material; increasing number of diatoms; some plant and algal material				
8-9 cm	Mostly inorganic material; increasing number of diatoms; some plant and algal material				
9-10 cm	Mostly inorganic material; increasing number of diatoms; some plant and algal material				
10-11 cm	Mostly inorganic material; small number of diatoms; some plant and algal material				

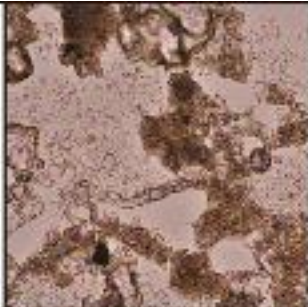
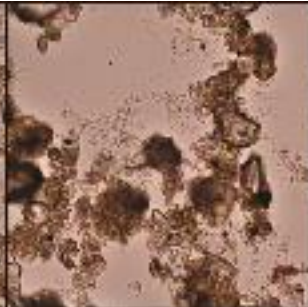
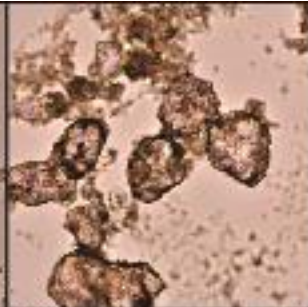
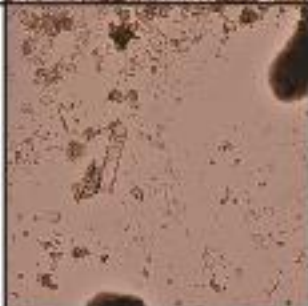
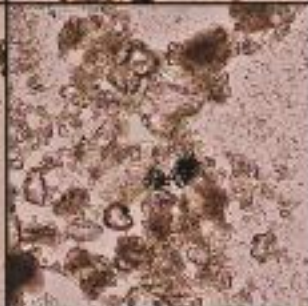
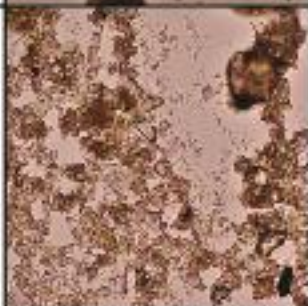
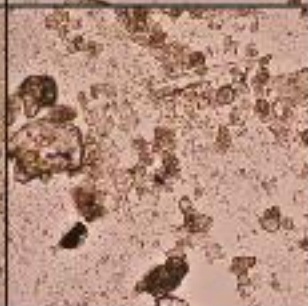
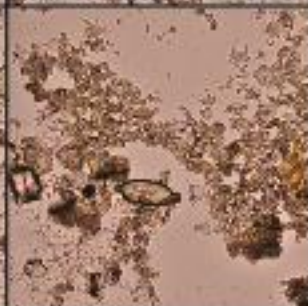
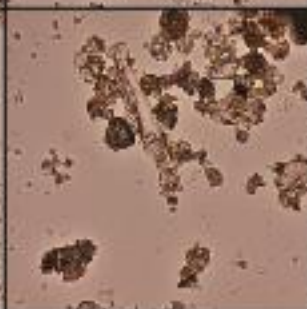
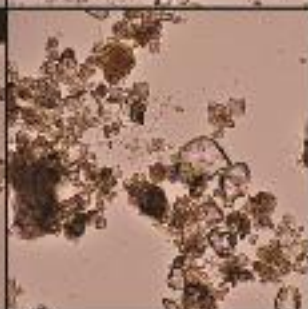
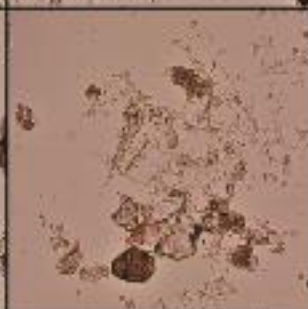
3-4 cm	Mostly inorganic material; high number of diatoms; some plant and algal material				
4-5 cm	Mostly inorganic material; high number of diatoms; some plant and algal material				
5-6 cm	Mostly inorganic material; high number of diatoms; some plant and algal material				
6-7 cm	Mostly inorganic material; high number of diatoms; some plant and algal material				

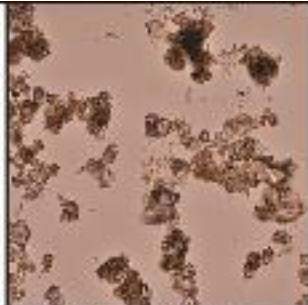
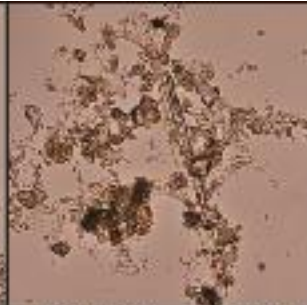
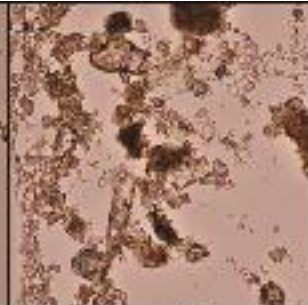
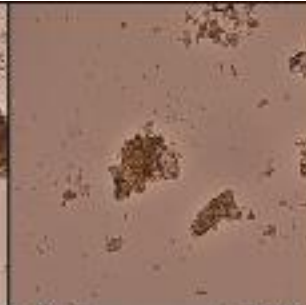
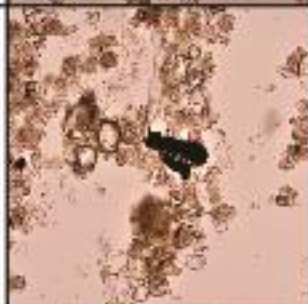
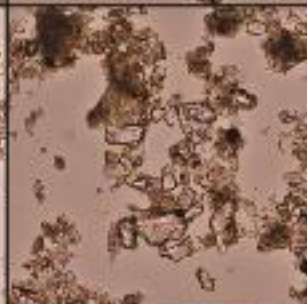
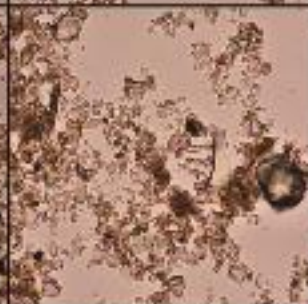
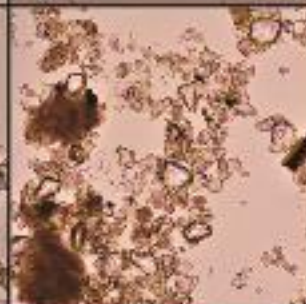
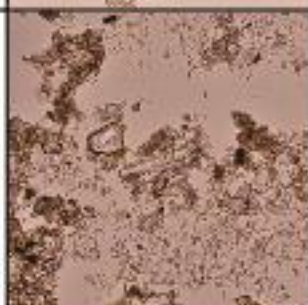
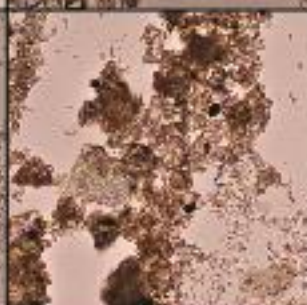
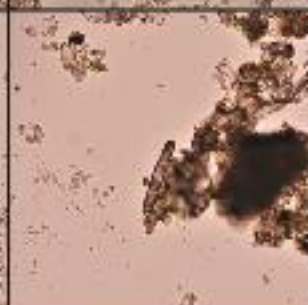
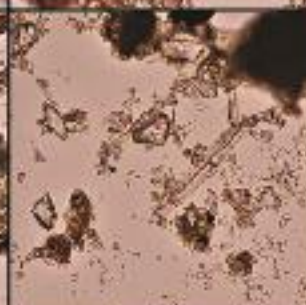
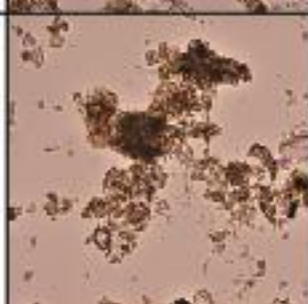
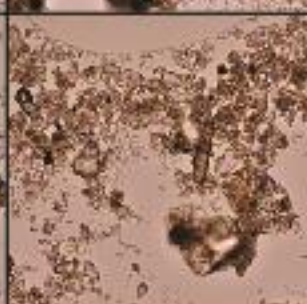
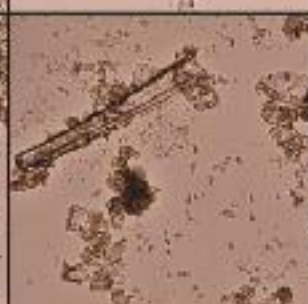
11-12 cm	Mostly inorganic material; small number of diatoms; some plant and algal material				
12-13 cm	Mostly inorganic material; diatoms reappear in small number; some plant and algal material				
13-14 cm	Mostly inorganic material; no diatoms some plant and algal material				
14-15 cm	Mostly inorganic material; no diatoms some plant and algal material				

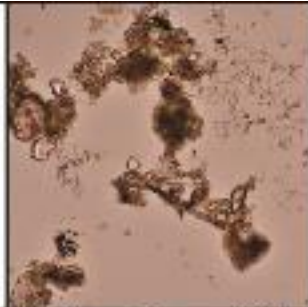
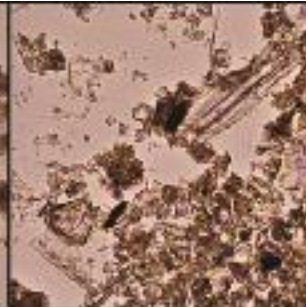
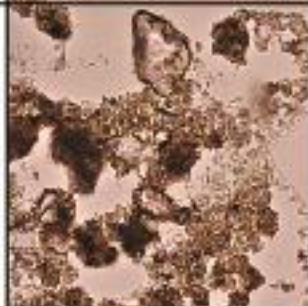
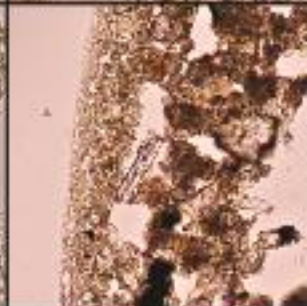
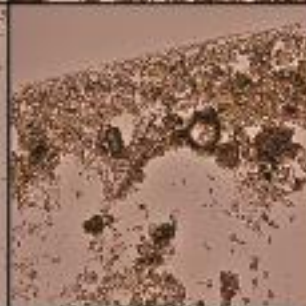
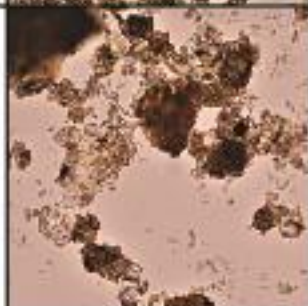
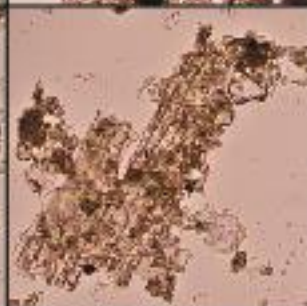
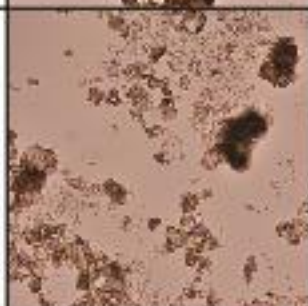
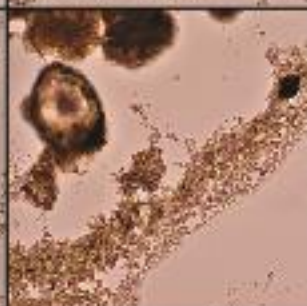
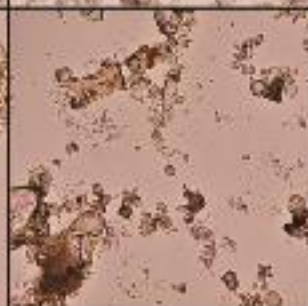
15-16 cm	Mostly inorganic material; no diatoms some plant and algal material				
16-17 cm	Mostly inorganic material; no diatoms some plant and algal material				
17-18 cm	Mostly inorganic material; no diatoms some plant and algal material				
18-19 cm	Mostly inorganic material; no diatoms some plant and algal material				

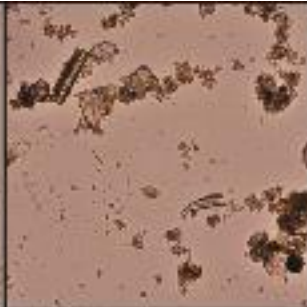
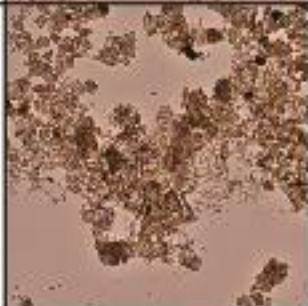
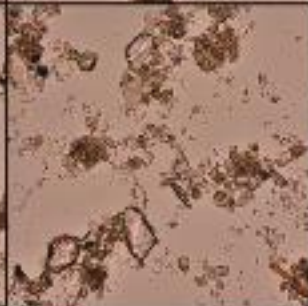
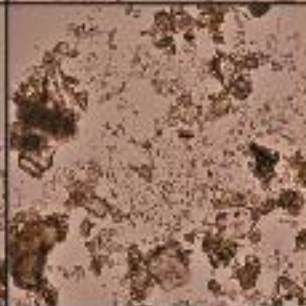
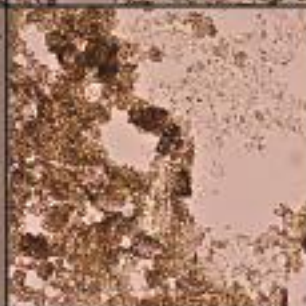
19-20 cm	Mostly inorganic material; no diatoms some plant and algal material				
20-21 cm	Mostly inorganic material; no diatoms some plant and algal material				
21-22 cm	Mostly inorganic material; no diatoms some plant and algal material				
22-23 cm	Mostly inorganic material; no diatoms some plant and algal material				

23-24 cm	Mostly inorganic material; no diatoms some plant and algal material				
24-25 cm	Mostly inorganic material; no diatoms some plant and algal material				
25-26 cm	Mostly inorganic material; no diatoms some plant and algal material				
26-27 cm	Mostly inorganic material; no diatoms some plant and algal material				

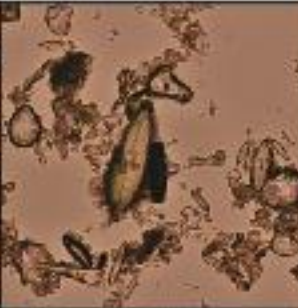
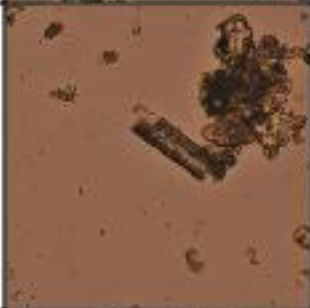
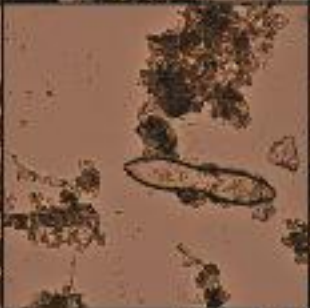
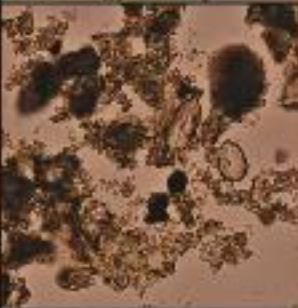
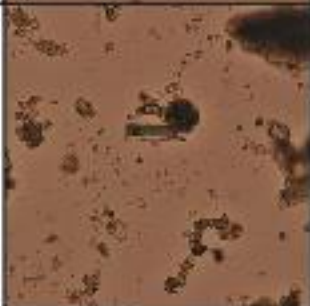
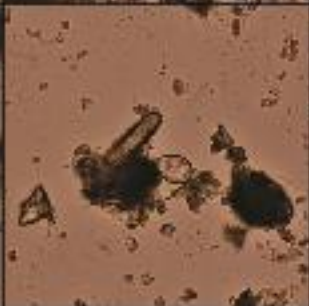
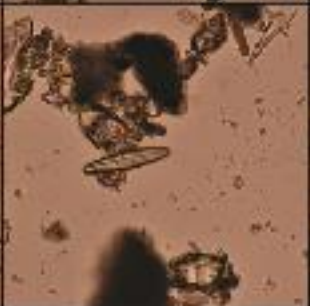
27-28 cm	Mostly inorganic material; diatoms disappear; some plant and algal material				
28-29 cm	Mostly inorganic material; small number of diatoms; some plant material				
29-30 cm	Mostly inorganic material; small number of diatoms; some plant material				
30-31 cm	Mostly inorganic material; small number of diatoms; some plant material				

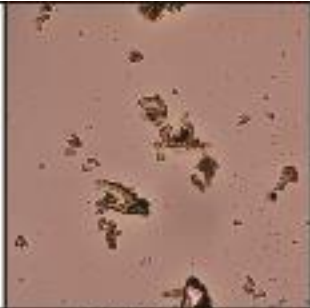
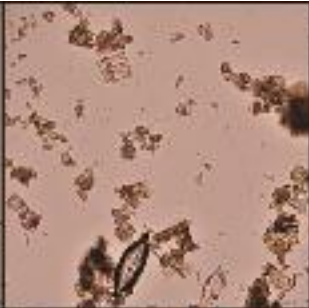
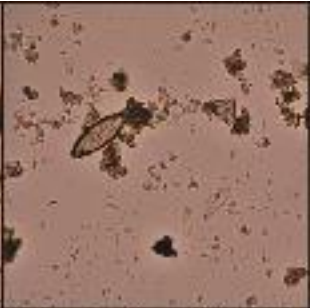
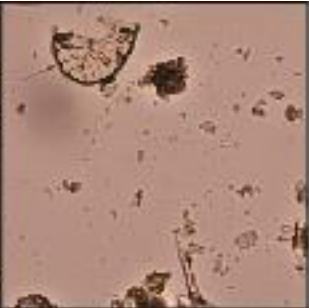
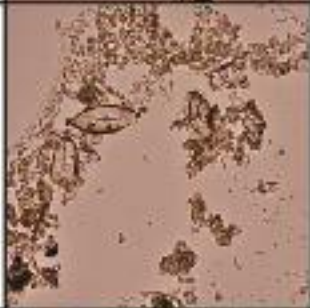
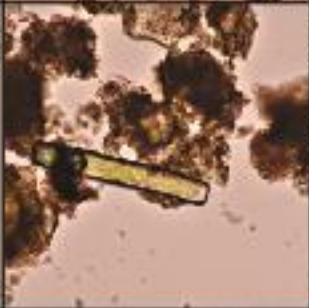
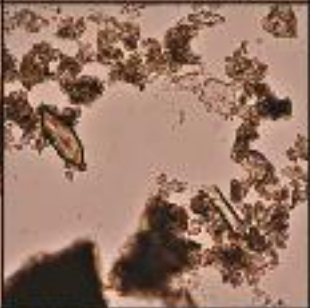
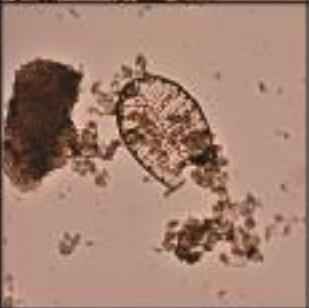
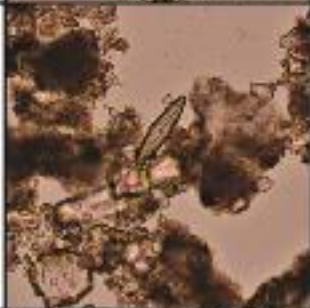
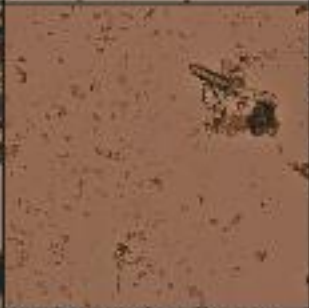
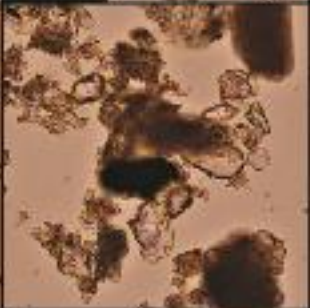
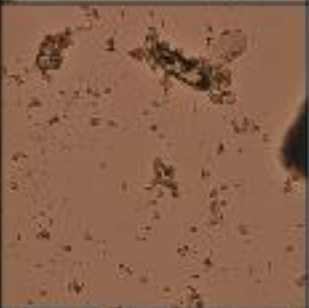
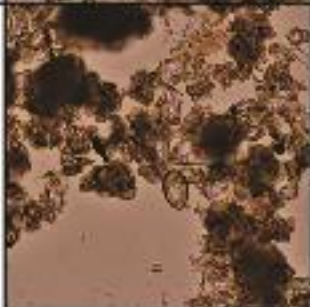
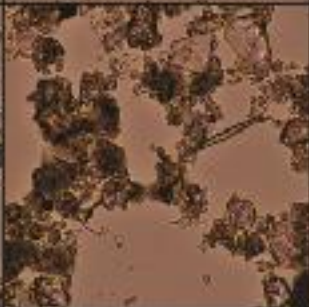
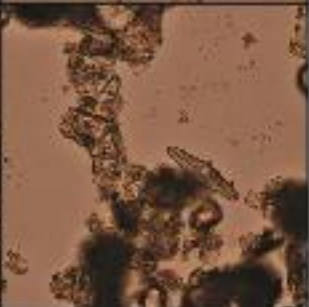
31-32 cm	Mostly inorganic material; small number of diatoms; some plant material				
32-33 cm	Mostly inorganic material; small number of diatoms; some plant material				
33-34 cm	Mostly inorganic material; small number of diatoms; some plant material				
34-35 cm	Mostly inorganic material; small number of diatoms; some plant material				

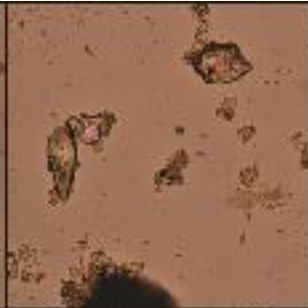
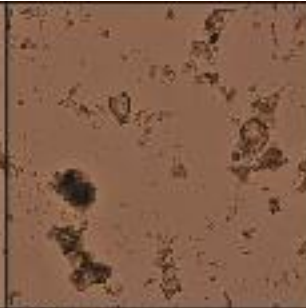
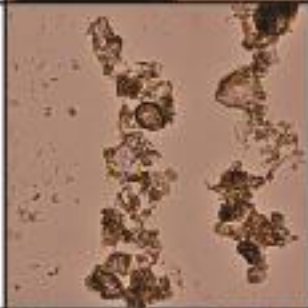
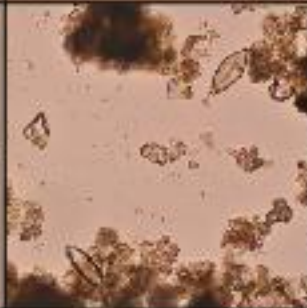
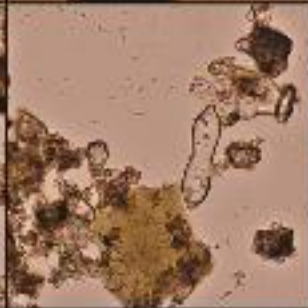
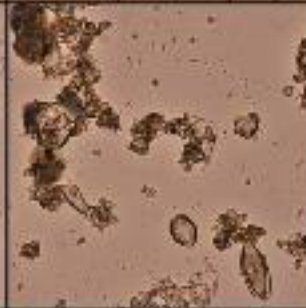
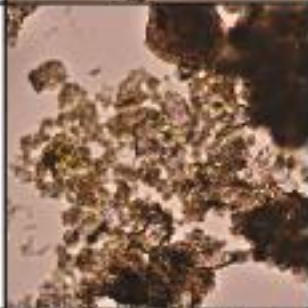
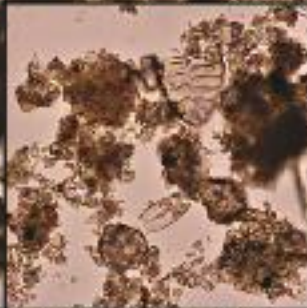
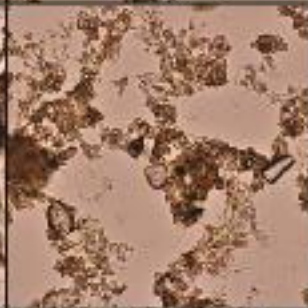
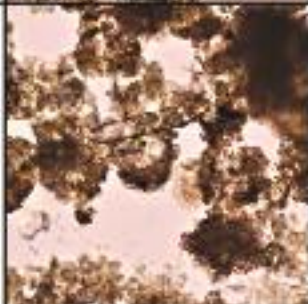
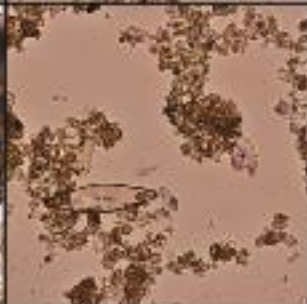
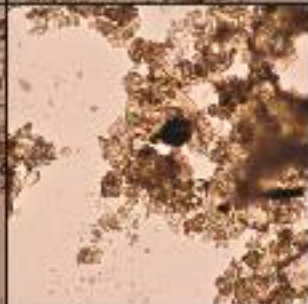
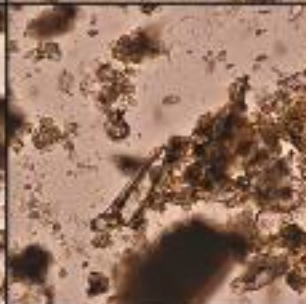
35-36 cm	Mostly inorganic material; small number of diatoms; some plant material				
36-37 cm	Mostly inorganic material; small number of diatoms; some plant material				
37-38 cm	Mostly inorganic material; small number of diatoms; some plant material				
38-39 cm	Mostly inorganic material; small number of diatoms; some plant material				

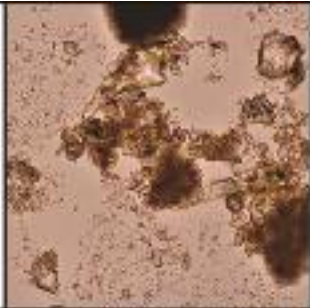
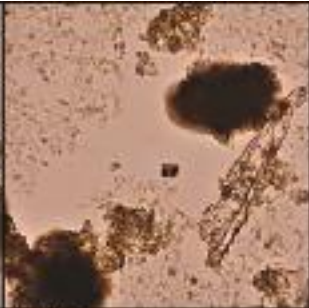
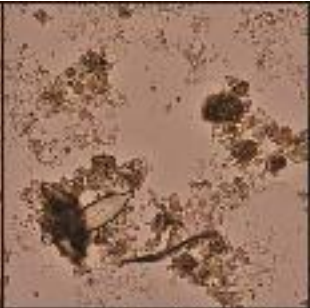
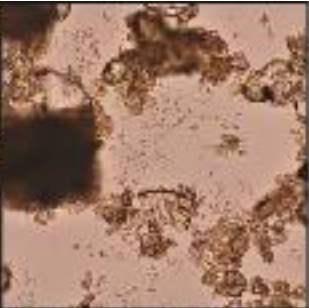
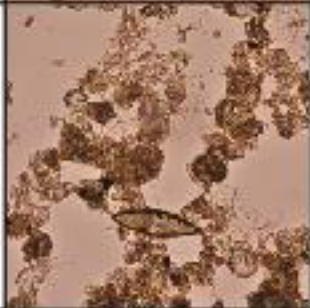
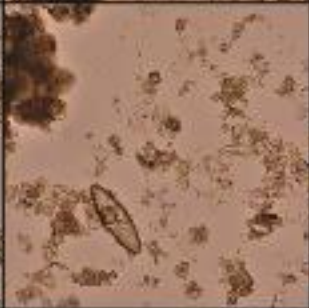
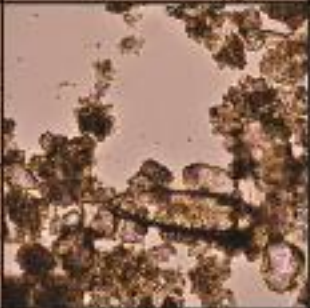
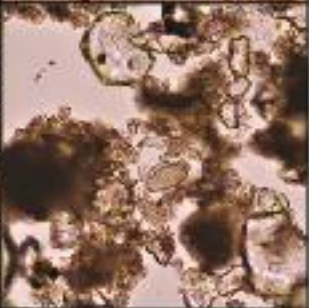
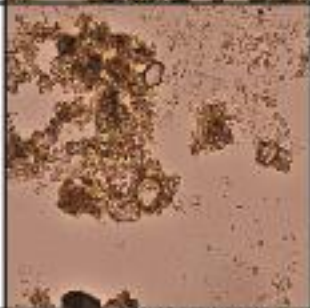
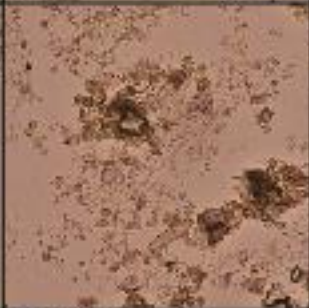
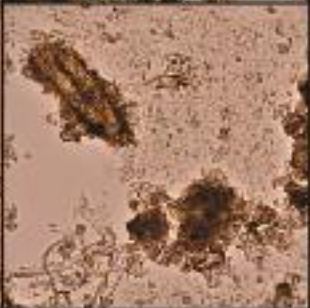
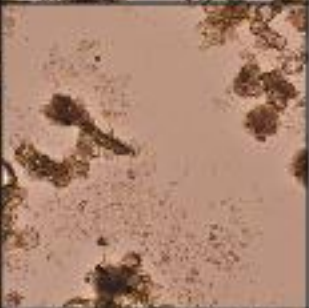
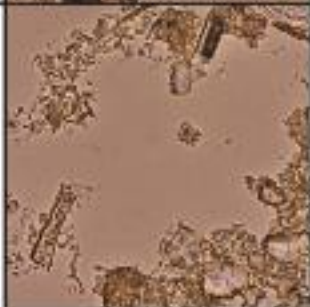
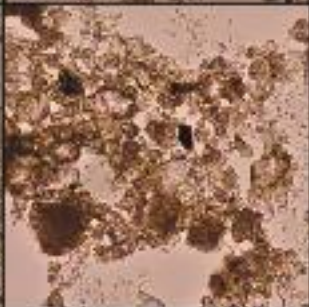
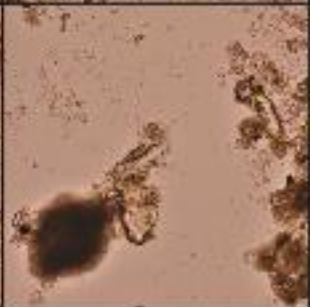
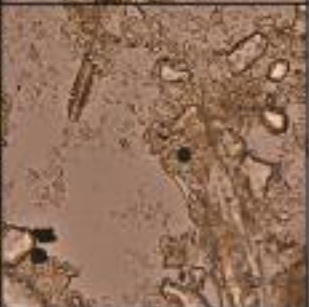
39-40 cm	Mostly inorganic material; small number of diatoms				
40-41 cm	Mostly inorganic material; small number of diatoms				
41-42 cm	Mostly inorganic material; small number of diatoms				

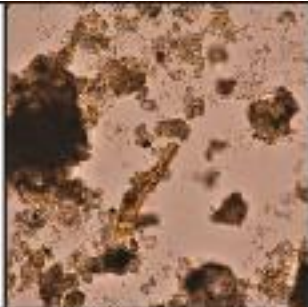
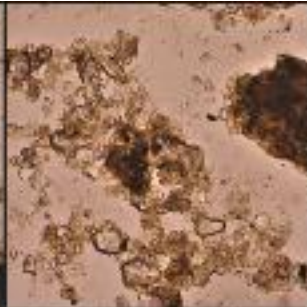
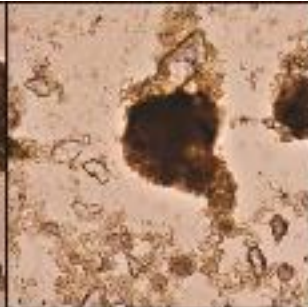
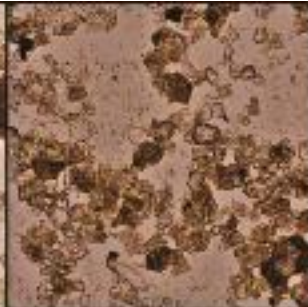
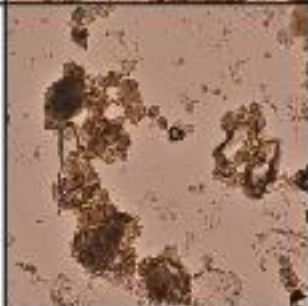
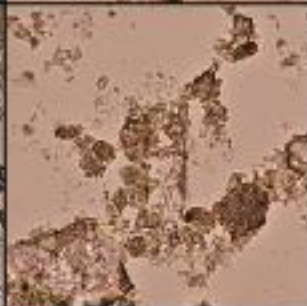
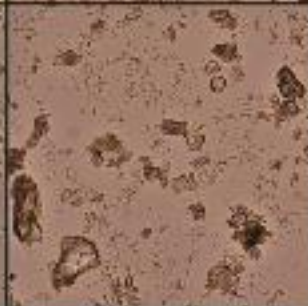
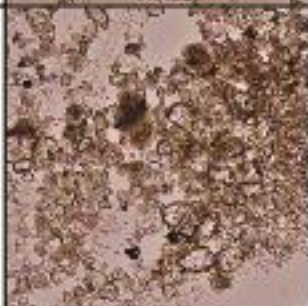
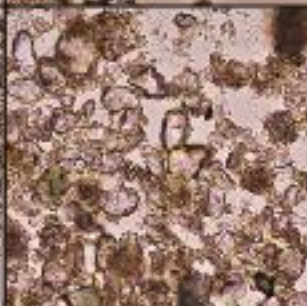
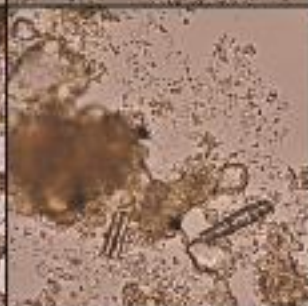
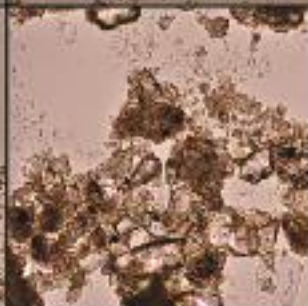
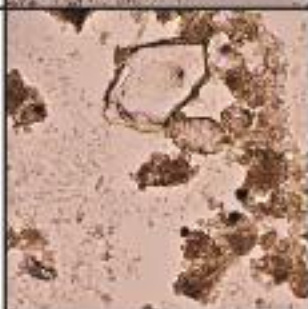
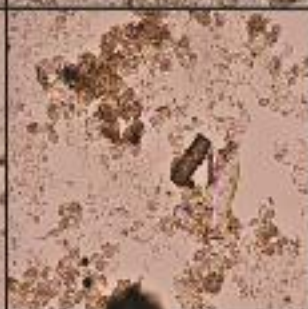
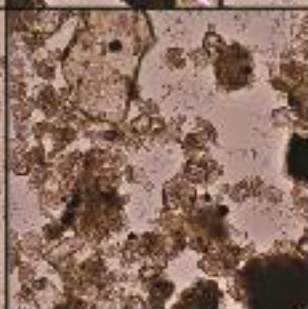
FB-2

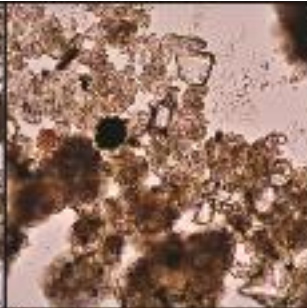
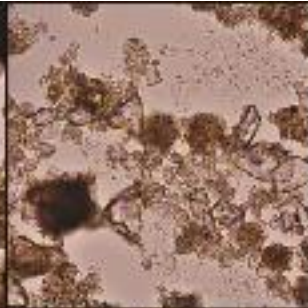
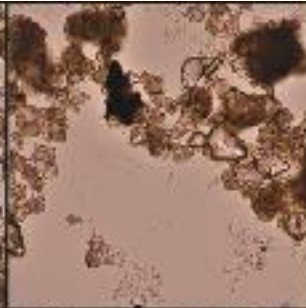
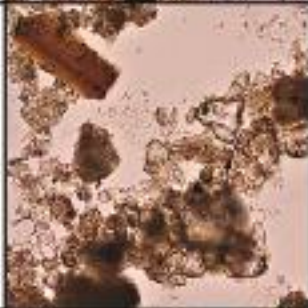
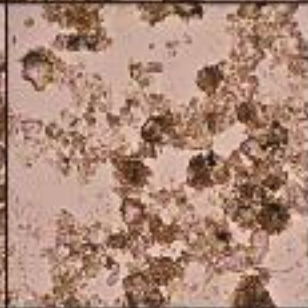
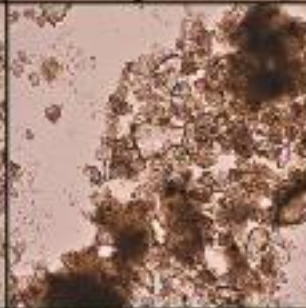
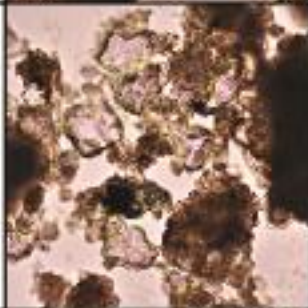
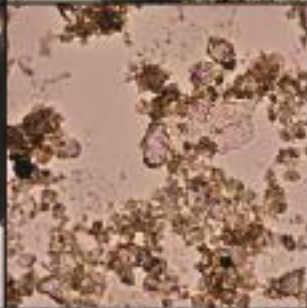
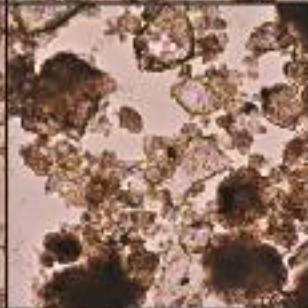
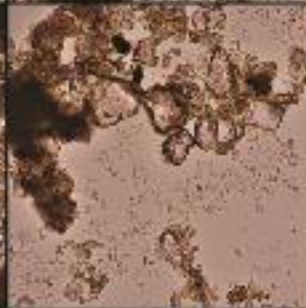
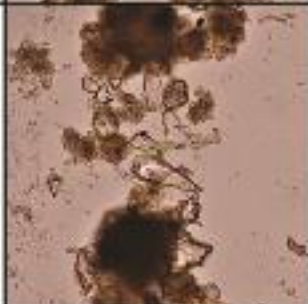
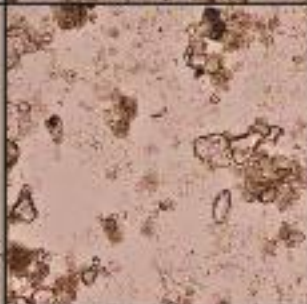
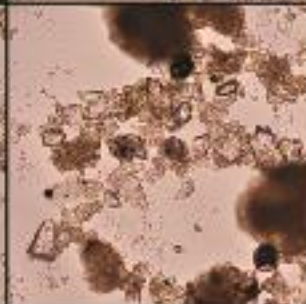
Depth	Description	Images			
0-1 cm	Mostly inorganic material; high number of diatoms; some plant and algal material				
1-2 cm	Mostly inorganic material; high number of diatoms; some plant and algal material				
2-3 cm	Mostly inorganic material; high number of diatoms; some plant and algal material				

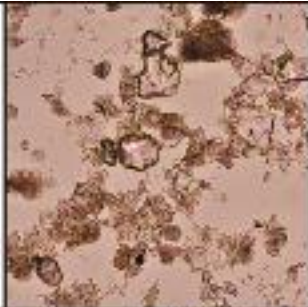
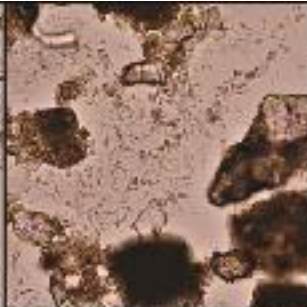
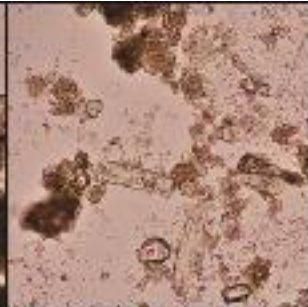
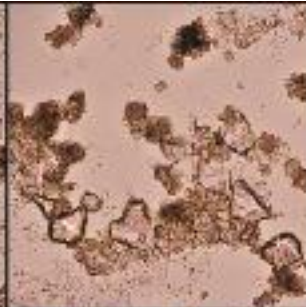
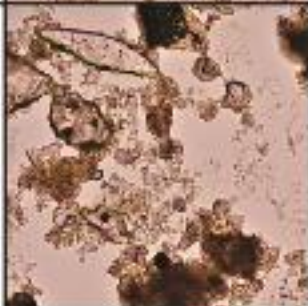
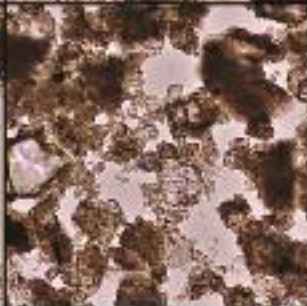
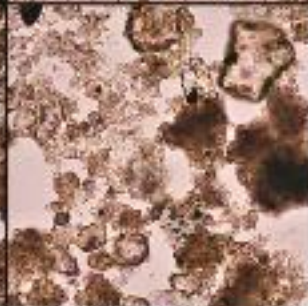
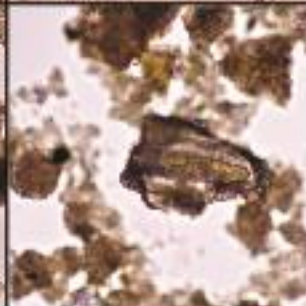
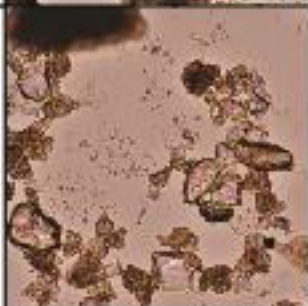
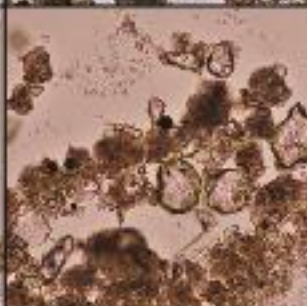
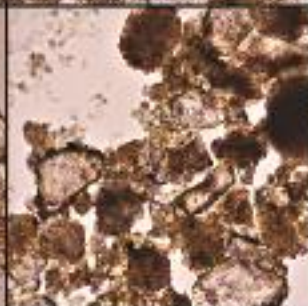
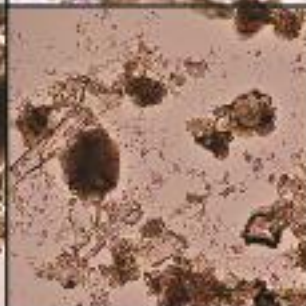
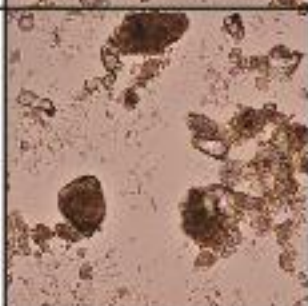
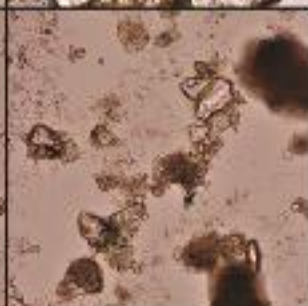
3-4 cm	Mostly inorganic material; high number of diatoms; some plant and algal material				
4-5 cm	Mostly inorganic material; high number of diatoms; some plant and algal material				
5-6 cm	Mostly inorganic material; high number of diatoms; some plant and algal material				
6-7 cm	Mostly inorganic material; high number of diatoms; some plant and algal material				

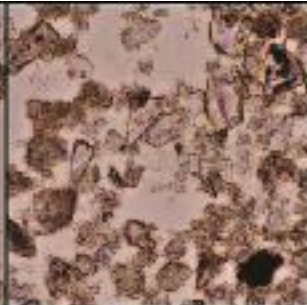
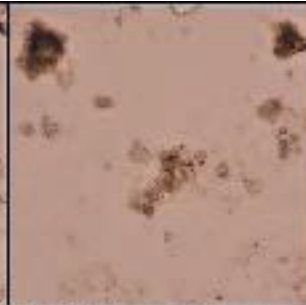
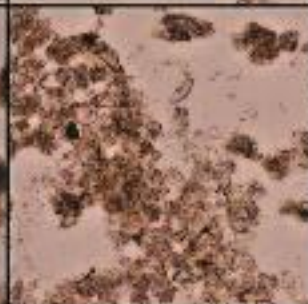
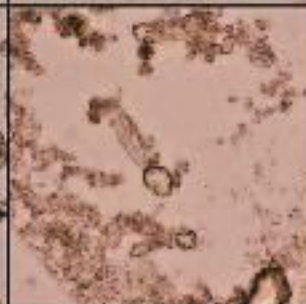
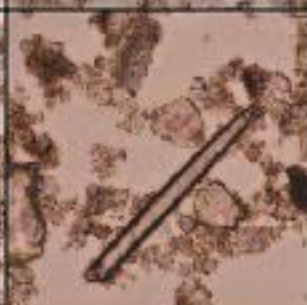
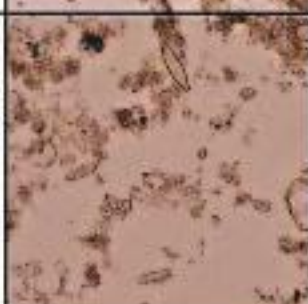
7-8 cm	Mostly inorganic material; high number of diatoms; some plant and algal material				
8-9 cm	Mostly inorganic material; high number of diatoms; some plant and algal material				
9-10 cm	Mostly inorganic material; increasing number of diatoms; some plant and algal material				
10-11 cm	Mostly inorganic material; increasing number of diatoms; some plant and algal material				

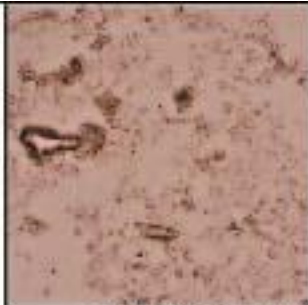
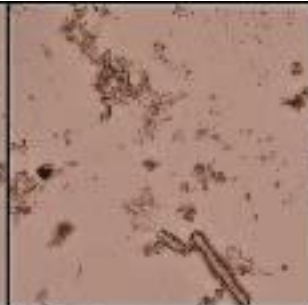
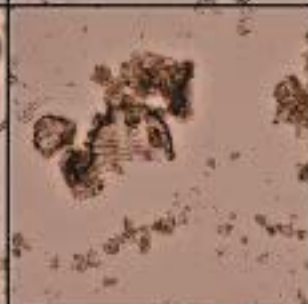
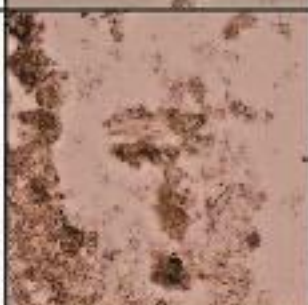
11-12 cm	Mostly inorganic material; increasing number of diatoms; some plant and algal material				
12-13 cm	Mostly inorganic material; small number of diatoms; some plant and algal material				
13-14 cm	Mostly inorganic material; small number of diatoms; some plant and algal material				
14-15 cm	Mostly inorganic material; small number of diatoms; some plant and algal material				

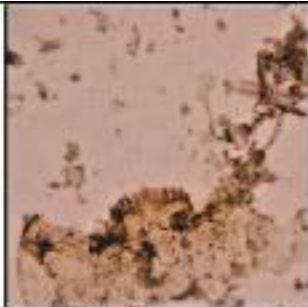
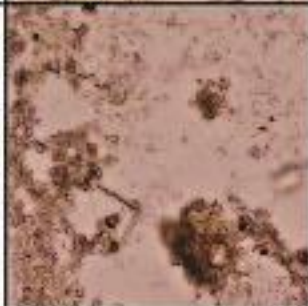
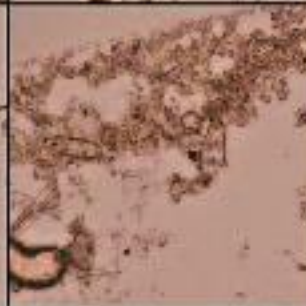
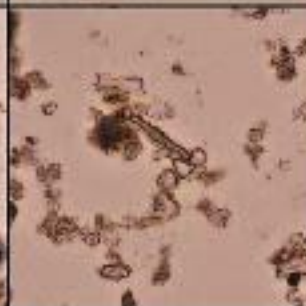
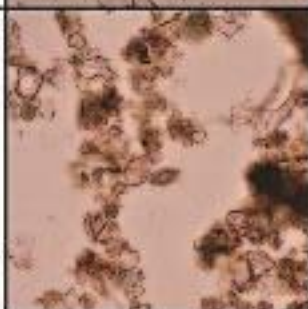
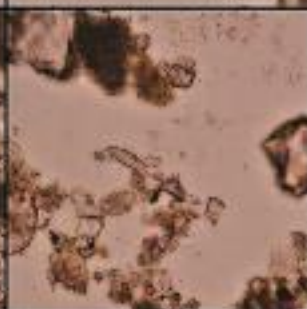
15-16 cm	Mostly inorganic material; small number of diatoms; some plant and algal material				
16-17 cm	Mostly inorganic material; small number of diatoms; some plant and algal material				
17-18 cm	Mostly inorganic material; diatoms reappear; some plant and algal material				
18-19 cm	Mostly inorganic material; no diatoms; some plant and algal material; pollen				

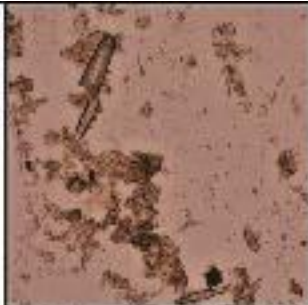
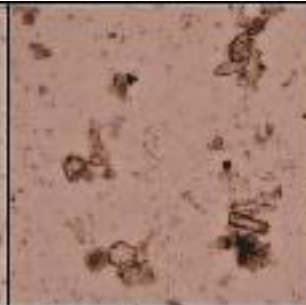
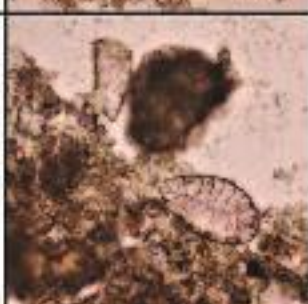
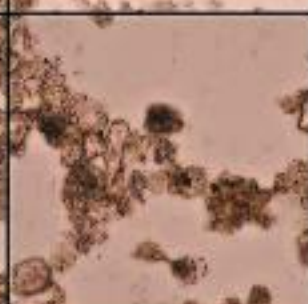
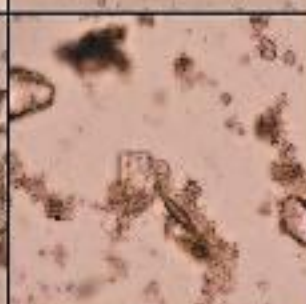
19-20 cm	Mostly inorganic material; small number of diatoms; some plant and algal material				
20-21 cm	Mostly inorganic material; no diatoms; some plant and algal material				
21-22 cm	Mostly inorganic material; small number of diatoms; some plant and algal material				
22-23 cm	Mostly inorganic material; small number of diatoms; some plant and algal material				

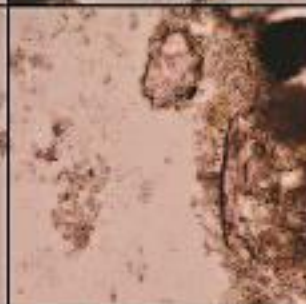
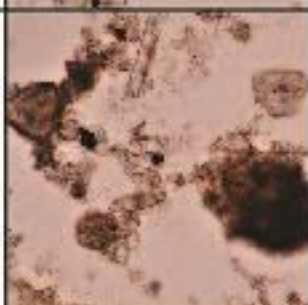
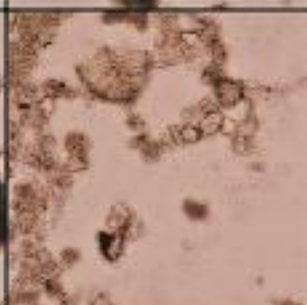
23-24 cm	Mostly inorganic material; small number of diatoms; some plant and algal material				
24-25 cm	Mostly inorganic material; small number of diatoms; some plant and algal material				
25-26 cm	Mostly inorganic material; no diatoms; some plant and algal material				
26-27 cm	Mostly inorganic material; small number of diatoms; some plant and algal material; pollen				

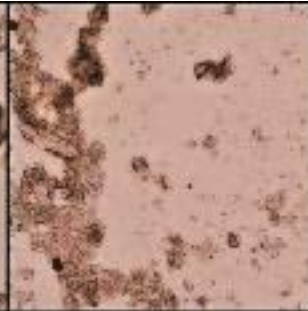
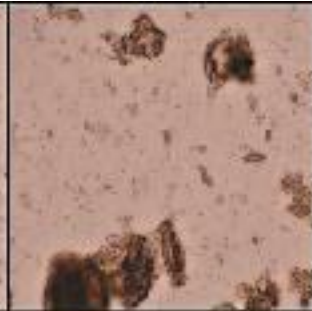
27-28 cm	Mostly inorganic material; small number of diatoms; some plant material				
28-29 cm	Mostly inorganic material; small number of diatoms; some plant material				
29-30 cm	Mostly inorganic material; small number of diatoms; some plant material				
30-31 cm	Mostly inorganic material; small number of diatoms; some plant material				

31-32 cm	Mostly inorganic material; small number of diatoms; some plant material				
32-33 cm	Mostly inorganic material; small number of diatoms; some plant material				
33-34 cm	Mostly inorganic material; small number of diatoms; some plant material				
34-35 cm	Mostly inorganic material; small number of diatoms; some plant material				

35-36 cm	Mostly inorganic material; small number of diatoms; some plant material; insects				
36-37 cm	Mostly inorganic material; small number of diatoms; some plant material				
37-38 cm	Mostly inorganic material; small number of diatoms; some plant material				
38-39 cm	Mostly inorganic material; small number of diatoms; some plant material				

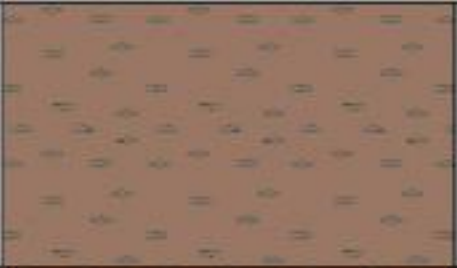
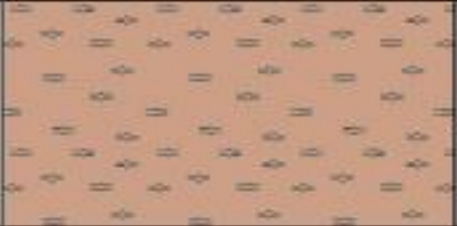
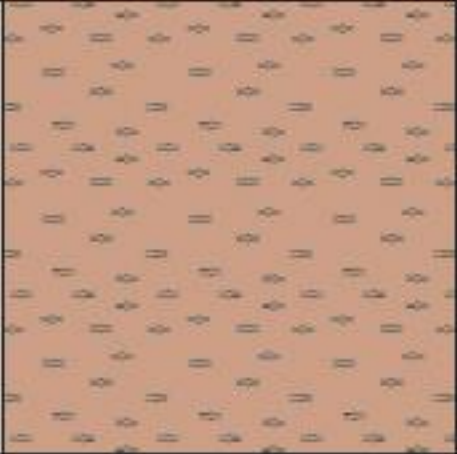
39-40 cm	Mostly inorganic material; small number of diatoms; some plant material				
40-41 cm	Mostly inorganic material; small number of diatoms; some plant material				
41-42 cm	Mostly inorganic material; small number of diatoms; some plant material				
42-43 cm	Mostly inorganic material; small number of diatoms; some plant material				

43-44 cm	Mostly inorganic material; small number of diatoms; some plant material				
44-45 cm	Mostly inorganic material; small number of diatoms; some plant material				
45-46 cm	Mostly inorganic material; small number of diatoms; some plant material				
46-47 cm	Mostly inorganic material; small number of diatoms; some plant material				

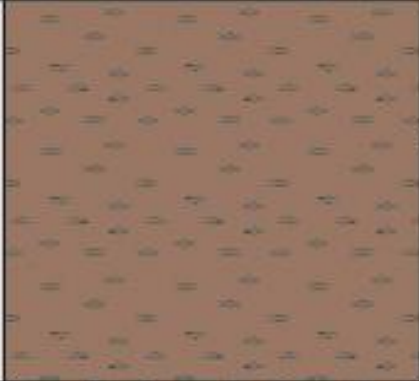
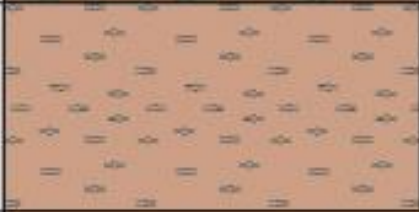
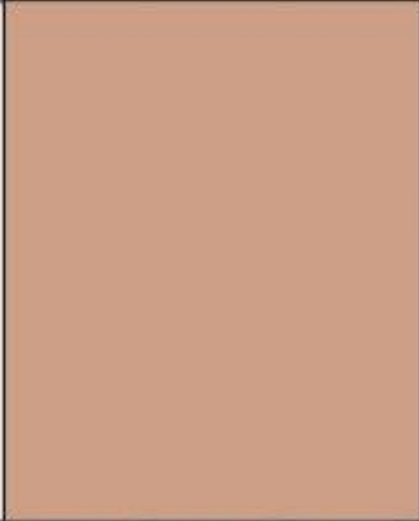
47-48 cm	Mostly inorganic material; small number of diatoms; some plant material				
----------	-------------------------------------------------------------------------	-----------------------------------------------------------------------------------	------------------------------------------------------------------------------------	-------------------------------------------------------------------------------------	-------------------------------------------------------------------------------------

Appendix C

FB-1

7 cm		Dark colored sediment; high number of diatoms; quartz, albite, calcium carbonate and clay composition
6 cm		Light colored sediment; medium number of diatoms; quartz, albite, calcium carbonate and clay composition
4 cm		Medium colored sediment; no diatoms; quartz, albite, calcium carbonate and high clay composition
13 cm		Light colored sediment; no diatoms; quartz, albite, calcium carbonate and clay composition
12 cm		Light colored sediment with dark streaks; low number of diatoms; quartz, albite, calcium carbonate and clay composition

FB-2

<p>11 cm</p>		<p>Dark colored sediment with even darker streaks, high number of diatoms; quartz, albite, calcium carbonate and clay composition</p>
<p>6 cm</p>		<p>Light sediment; medium number of diatoms; quartz, albite, calcium carbonate, and clay composition</p>
<p>15 cm</p>		<p>Light colored sediment; burrow marks, little to no diatoms; quartz and clay composition with a high amount of calcite</p>
<p>16 cm</p>		<p>Medium colored sediment; medium number of diatoms; quartz, albite, calcium carbonate and clay composition</p>

Appendix D

Table 2. UTM coordinates of coring sites.

	Easting	Northing
FB-1	411269	4529700
FB-2	418353	4534095